

Coupled Thermal-Mechanical Modelling of a Deep Geological Repository using the Horizontal Tunnel Placement Method in Sedimentary Rock using CODE_BRIGHT

NWMO TR-2010-22

December 2010

Ruiping Guo

Atomic Energy of Canada Limited

nwmo

NUCLEAR WASTE
MANAGEMENT
ORGANIZATION

SOCIÉTÉ DE GESTION
DES DÉCHETS
NUCLÉAIRES



Nuclear Waste Management Organization
22 St. Clair Avenue East, 6th Floor
Toronto, Ontario
M4T 2S3
Canada

Tel: 416-934-9814
Web: www.nwmo.ca

**Coupled Thermal-Mechanical Modelling of a Deep Geological Repository using the
Horizontal Tunnel Placement Method in Sedimentary Rock using CODE_BRIGHT**

NWMO TR-2010-22

December 2010

Ruiping Guo
Atomic Energy of Canada Limited

Disclaimer:

This report does not necessarily reflect the views or position of the Nuclear Waste Management Organization, its directors, officers, employees and agents (the "NWMO") and unless otherwise specifically stated, is made available to the public by the NWMO for information only. The contents of this report reflect the views of the author(s) who are solely responsible for the text and its conclusions as well as the accuracy of any data used in its creation. The NWMO does not make any warranty, express or implied, or assume any legal liability or responsibility for the accuracy, completeness, or usefulness of any information disclosed, or represent that the use of any information would not infringe privately owned rights. Any reference to a specific commercial product, process or service by trade name, trademark, manufacturer, or otherwise, does not constitute or imply its endorsement, recommendation, or preference by NWMO.

ABSTRACT

Title: Coupled Thermal-Mechanical Modelling of a Deep Geological Repository using the Horizontal Tunnel Placement Method in Sedimentary Rock using CODE_BRIGHT
Report No.: NWMO TR-2010-22
Author(s): Ruiping Guo
Company: Atomic Energy of Canada Limited
Date: December 2010

Abstract

A series of three-dimensional thermal transient and thermal-mechanical (T-M) stress analyses was performed on a deep geological repository (DGR) for used CANDU fuel using the Horizontal Tunnel Placement (HTP) geometry. The DGR modelled in this document is assumed to be located at a depth of 500 m in limestone.

Based on the near-field modelling, the peak temperature of the container surface is 117.0°C at 10 years after used fuel placement and the peak temperature of the tunnel surface is 69.0°C at 50 years after used fuel placement.

A coupled near-field T-M model was conducted for the first 1,000 years after placement of the used fuel in a DGR. Excavation-induced mechanical stresses in the rock around the placement tunnel were studied.

The stability of the rock mass was evaluated using the modified Hoek and Brown empirical failure criterion. Excavation of the placement tunnel could potentially cause a damage zone with a thickness of 0.053 m near the placement tunnel roof. At 1,000 years after placement, this damage zone in the tunnel roof will extend to a depth of 0.211 m from the tunnel roof's original surface. At the same time, a layer of damaged rock with a thickness of 0.077 m could potentially develop on the tunnel wall.

Coupled T-M far-field analyses were used to determine the peak temperatures at various regions in the repository. The peak temperature in the rock is 42.7°C at the centre of the repository after 1,200 years. The peak temperatures at the centre of the repository edge (727.5 m from repository centreline) and repository corner (1,265 m from repository centreline) are 27.6°C and 20.3°C, respectively, at 4,000 years after placement. These analyses determined that the maximum thermally induced uplift at the ground surface above the centre of the repository would be about 0.13 m. This degree of deformation was determined not to be sufficient to generate additional fractures in the rock near the ground surface.

TABLE OF CONTENTS

	<u>Page</u>
ABSTRACT	v
1. INTRODUCTION	1
2. DESCRIPTION OF A PROPOSED DEEP GEOLOGICAL REPOSITORY, GEOSPHERE AND MATERIAL PARAMETERS	2
2.1 DESCRIPTION OF A PROPOSED DEEP GEOLOGICAL REPOSITORY	2
2.2 ASSUMPTIONS	4
2.3 MATERIAL PROPERTIES	5
3. NEAR-FIELD MODELLING	8
3.1 NEAR-FIELD THERMAL MODELLING	8
3.1.1 Geometry	8
3.1.2 Boundary Conditions and Initial Conditions	8
3.1.3 Thermal Results from the Near-field Thermal Model	11
3.2 Near-Field Coupled T-M Modelling	15
3.2.1 Model Geometry, Boundary Conditions and Initial Conditions	15
3.2.2 Thermal Results from the Coupled T-M Model	19
3.2.3 Mechanical Results from the Coupled T-M Model	20
3.2.4 Stability Analyses	24
3.2.5 Summary of the Results from Near-field Coupled T-M Model	25
4. FAR-FIELD MODELLING	26
4.1 FAR-FIELD MODEL GEOMETRY, BOUNDARY CONDITIONS AND INITIAL CONDITIONS	26
4.1.1 Far-Field Model Geometry and Material Parameters	26
4.1.2 Far-field Model Boundary Conditions and Initial Conditions	28
4.1.2.1 Thermal Boundary Conditions of the Far-Field Model	28
4.1.2.2 Mechanical Boundary Conditions of the Far-Field Model	28
4.1.3 Initial Conditions for the Far-field Modelling	29
4.1.4 Finite Element Discretization	30
4.2 RESULTS FROM FAR-FIELD MODEL	30
4.2.1 Thermal Results from Far-Field Model	31
4.2.2 Mechanical Results from Far-Field Model	37
4.2.2.1 Thermally Induced Vertical Displacements	37
4.2.2.2 Thermally Induced Stresses	41
4.2.2.3 Total Stresses	45
4.2.3 Summary of Far-field T-M Modelling of Repository	51
5. SUMMARY OF THE RESULTS	52
ACKNOWLEDGEMENTS	53
REFERENCES	54

LIST OF TABLES

	<u>Page</u>
Table 1: Geomechanical Properties for the Shale, Limestone and Granite.....	4
Table 2: Heat Output of Containers of Used CANDU Fuel at Different Times	7
Table 3: Thermal and Mechanical Properties of the Bentonite Buffer Pellets	8

LIST OF FIGURES

	<u>Page</u>
Figure 1: Layout of a Proposed Deep Geological Repository in Sedimentary Rock using the HTP Method (SNC-Lavalin 2010).....	3
Figure 2: Lithostratigraphic Column – Limestone Geosphere (after SNC-Lavalin (2010)) (drawing not to scale)	5
Figure 3: Geometry of the HTP Method.....	6
Figure 4: Dimensions and Meshes of the Near-Field Model	10
Figure 5: Temperatures at Different Locations along Horizontal Line FCD (see Figure 4 for the location of this line).....	11
Figure 6: Temperatures along Horizontal Line FCD (see Figure 4 for location) at Seven Different Times.....	12
Figure 7: Temperatures at Different Locations along Vertical Line BA (see Figure 4 for the location of this line).....	13
Figure 8: Temperatures along Vertical Line BA at Seven Different Times (see Figure 4 for the location of this line).....	13
Figure 9: Temperatures at Four Locations along Tunnel Roof BE (see Figure 4 for the location of the line of BE).....	14
Figure 10: Temperature along Tunnel Roof BE at Six Different Times	14
Figure 11: Temperature Contours in the Rock surrounding the Buffer.....	15
Figure 12: Temperature Contours in the Buffer at Four Different Times	16
Figure 13: Geometry and Meshes for the Coupled T-M Near-field Model.....	17
Figure 14: Thermal Boundary Conditions of the Coupled T-M Model	18
Figure 15: Comparison of Temperature at Three Different Locations along Horizontal Line FCD between Thermal Only Model (T-) and Coupled T-M Model (TM-)	19
Figure 16: X-Directional Stresses along Vertical Line BA	20
Figure 17: Y-Directional Stresses along Vertical Line BA	21
Figure 18: Z-Directional Stresses along Vertical Line BA	21
Figure 19: X-Directional Stress along Horizontal Line CD	22
Figure 20: Y-Directional Stress along Horizontal Line CD	23
Figure 21: Z-Directional Stress along Horizontal Line CD	23
Figure 22: Safety Factors along Vertical Line BA	24
Figure 23: Safety Factors along Horizontal Line CD.....	25
Figure 24: Geometry for the Coupled T-M Far-Field Model	27
Figure 25: Thermal Boundary Conditions for Far-Field Coupled T-M Model.....	28
Figure 26: Mechanical Boundary Conditions for Far-Field Coupled T-M Model	29
Figure 27: Meshes for the Far-Field Coupled T-M Model	30
Figure 28: Temperatures at Three Different Locations of Points O, P and Q (for location see Figure 24).....	31
Figure 29: Temperatures versus Distances from Repository Centre along Horizontal Line OR through the Repository Model (for location see Figure 24).....	32

Figure 30: Temperatures along Vertical Line AE (for location see Figure 24) at 5 Times following Repository Closure	33
Figure 31: Thermally Induced Temperature Rise along Vertical Line AE (for location see Figure 24) at 5 Times following Repository Closure.....	34
Figure 32: Temperature Rise induced only by Used Nuclear Fuel in a Repository at Different Depths below Ground Surface along Vertical Line AE (for location see Figure 25).....	35
Figure 33: Temperature Response at 6 Different Times (The base of these figures is located at 2812 m below ground surface)	36
Figure 34: Vertical Displacements versus Time at Different Locations along Vertical Line AE running through the Repository (for location see Figure 24)	37
Figure 35: Vertical Displacements along Vertical Line AE (for location see Figure 24) at Different Times.....	38
Figure 36: Vertical Displacements at Points A, P', and B of Repository Site (see Figure 24 for locations).....	39
Figure 37: Vertical Displacements along Line AB at Different Times (see Figure 24 for location of this line at the repository site).....	39
Figure 38: Thermally Induced Vertical Displacements at 5000 Years with a Maximum Value of 0.14 m (Note: The vertical displacement scale is exaggerated (factor = 5,000) for clarity)	40
Figure 39: Thermally Induced Stresses in X-direction along Horizontal Line OR at Repository Level (for location see Figure 24)	41
Figure 40: Thermally Induced Stresses in Y-direction along Horizontal Line OR at Repository Level (for location see Figure 24)	42
Figure 41: Thermally Induced Stresses in Z-direction along Horizontal Line OR at Repository Level (for location see Figure 24)	42
Figure 42: Thermally Induced Stresses in X-direction along Vertical Line AE through Repository (for location see Figure 24).....	43
Figure 43: Thermally Induced Stresses in Y-direction along Vertical Line AE through Repository Centreline (see Figure 24 for location).....	44
Figure 44: Thermally Induced Stresses in Z-direction along Vertical Line AE through Repository Line (see Figure 24 for location)	45
Figure 45: Total Stresses in X-direction along Horizontal Line OR (see Figure 24 for location) at Different Times	46
Figure 46: Total Stresses in Y-direction along Horizontal Line OR (see Figure 24 for location) at Different Times	46
Figure 47: Total Stresses in Z-direction along Horizontal Line OR (see Figure 24 for location) at Different Times	47
Figure 48: Total Stresses in X-direction along Vertical Line (AE in Figure 24) at Different Times	48
Figure 49: Total Stresses in Y-direction along Vertical Line (AE in Figure 24) at Different Times	49
Figure 50: Total Stresses in Z-direction along Vertical Line (AE in Figure 24) at Different Times	50
Figure 51: Rock Mass Strength versus Depth from the Ground Surface	51

1. INTRODUCTION

The Nuclear Waste Management Organization (NWMO) is implementing the Adaptive Phased Management (APM) approach accepted by the Government of Canada (NRCan 2007) for the long-term management of Canada's used nuclear fuel. APM has, as its end point, the containment and isolation of used fuel in a deep geological repository (DGR) constructed in a suitable host rock formation such as crystalline or sedimentary rock (NWMO 2005). The Precambrian crystalline rock of the Canadian Shield and Paleozoic sedimentary rock are considered to be potential host geologic media in the current Canadian DGR conceptual design studies.

Sedimentary rock is being studied by some international nuclear waste management organizations (e.g., NAGRA, ANDRA, ONDRAF/NIRAS) as the host medium for their DGRs. NAGRA has proposed a Horizontal Tunnel Placement (HTP) geometry for a used-fuel/high-level waste repository (NAGRA 1985; NAGRA 2002). A scoping-level investigation was performed by Baumgartner (2005) to assess the feasibility of applying a NAGRA-type HTP geometry for a DGR for Canadian used nuclear fuel in Ordovician shale and limestone sedimentary formations in Canada.

In this study, both near-field and far-field thermal-mechanical (T-M) analyses are performed to assess thermally acceptable repository layouts, mechanical stability of the near-field rock at the walls of the placement tunnel, and evolution of the thermal response for various locations in a DGR. In order to further develop the Canadian capability for modelling using CODE_BRIGHT, CODE_BRIGHT (CODE_BRIGHT_v 3beta) is used to assess the thermal and mechanical response of a DGR in limestone using the HTP method at an assumed depth of 500 m below ground surface. This report describes the CODE_BRIGHT model and modelling results.

CODE_BRIGHT has been extensively used to conduct the THM modelling of DGRs in crystalline rock using the In-Floor Borehole (IFB) placement method. This placement method was developed to allow for placement of a used-fuel container in a borehole drilled in the floor of a tunnel excavated in crystalline rock. In 2007, an assessment of the thermal and mechanical simulation of the IFB used-fuel container placement method for a DGR in crystalline rock was performed using CODE_BRIGHT (Guo 2007). Sensitivity analyses were performed in 2008 to investigate the influence of the container spacing and placement-room spacing on the thermal response in a DGR located in limestone at an assumed depth of 750 m from the ground surface using the horizontal placement method, also using CODE_BRIGHT (Guo 2008). In 2009, CODE_BRIGHT was also used in choosing placement-room spacing, container spacing and placement-room shape and predicting the thermal-mechanical (T-M) response of a DGR in granite using the in-floor placement method at an assumed depth of 500-m below ground surface (Guo 2009). CODE_BRIGHT is a general-purpose finite element program for the analysis of coupled thermo-hydro-mechanical (THM) phenomena in geological media and developed by Universidad Politècnica de Catalunya (Olivella et al. 1996). GiD is a universal, adaptive and user-friendly graphical user interface for geometrical modelling, data input and visualization of results for all types of numerical simulation programs (<http://gid/cimne.upc.es>) and was developed by Universidad Politècnica de Catalunya. Version 9.0.6 of GiD is the version available at the time of preparing this document and is used for pre-processing of modelling input and post-processing of modelling results.

CODE_BRIGHT has been used to undertake an initial assessment of the HTP geometry in sedimentary rock and this report contains:

- a description of the modelled DGR scenario;
- material parameters;
- near-field thermal modelling and coupled T-M modelling;
- stability analyses;
- far-field thermal modelling and coupled T-M modelling; and
- summary and conclusions.

2. DESCRIPTION OF A PROPOSED DEEP GEOLOGICAL REPOSITORY, GEOSPHERE AND MATERIAL PARAMETERS

2.1 DESCRIPTION OF A PROPOSED DEEP GEOLOGICAL REPOSITORY

The overall dimension of an underground DGR at a depth of 500 m in limestone is 2,069 m by 1,455 m as shown in Figure 1 (SNC-Lavalin 2010). The geological conditions of the DGR are shown in Figure 2 and Table 1. The DGR has been designed to accommodate 11,000 used fuel containers (UFCs) and assumes that 10% of the space in the placement tunnel may potentially be rejected due to poor ground. Each container is 3,909-mm long with a diameter of 1,247 mm and will accommodate 360 fuel bundles. The container design consists of an outer copper corrosion-barrier shell and an inner, carbon steel load-bearing component (Maak and Simmons 2001).

The modelled DGR layout consists of an array of horizontal, circular-shaped placement tunnels, each of 2.5 m in diameter. The placement tunnels are connected by access tunnels for moving excavated rock, used-fuel containers and backfilling materials. These rooms are arranged into eight distinct panels. Each of the four panels on one side of repository access drifts 1 and 2 consist of 28 rooms (spaced at 20 m centre-to-centre) and each of the four panels on the other side of access drifts 1 and 2 consist of 27 rooms. Each room is designed to contain 50 UFCs. Each container is installed in the placement tunnel horizontally along the centreline of the tunnel at a centre-to-centre spacing of 8 m. As shown in Figure 3, the UFC rests on a highly compacted bentonite and is surrounded by particulate-bentonite buffer material in the placement tunnel. The centre-to-centre container spacing of 8 m and the tunnel spacing of 20 m were determined by near-field thermal analyses as part of this study (see Section 3.2). The thermal analyses were based on the criteria of a maximum temperature of 120°C on the external surface of the container (NMWO 2009).

Stresses around circular placement tunnels are influenced by the orientation of the placement tunnel relative to the major and minor principal stresses in the rock mass. In order to minimize the tangential stress concentrations around the room, the placement tunnel should be oriented such that its axis is parallel to the maximum principal stress direction.

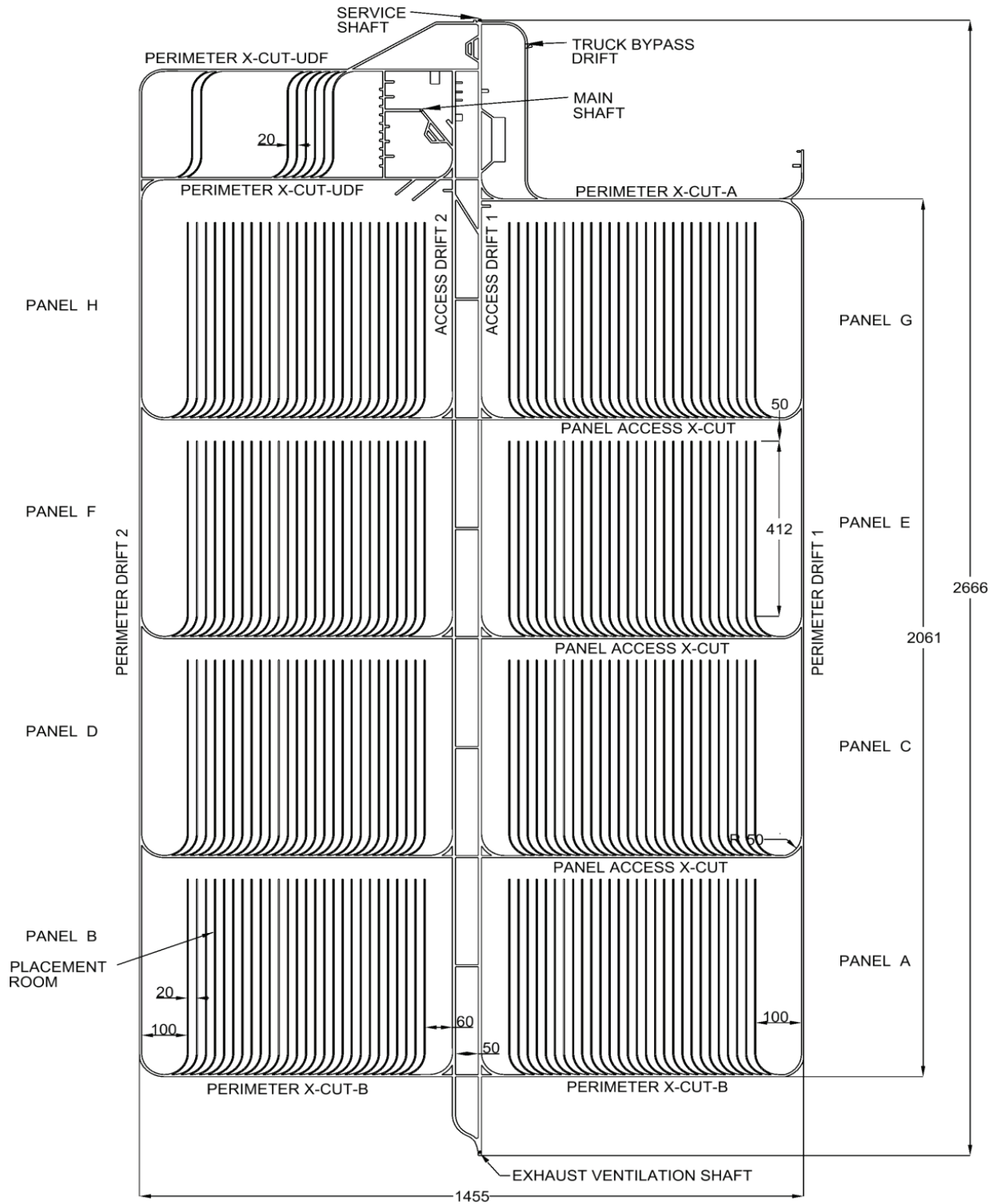


Figure 1: Layout of a Proposed Deep Geological Repository in Sedimentary Rock using the HTP Method (SNC-Lavalin 2010)

Table 1: Geomechanical Properties for the Shale, Limestone and Granite

Property	Shale	Limestone	Granite
Thermal conductivity (W/m°C)	2.1	2.3	3
Specific heat (J/kg°C)	975	830	845
Bulk density (kg/m ³)	2600	2600	2700
Dry density (kg/m ³)	2600	2600	2700
Porosity (%)	6-7	2	0.5
Young's modulus (GPa)	15	30	45
Poisson's ratio	0.3	0.3	0.25
In-situ stresses (MPa)	$\sigma_1 = 0.0303 \cdot z + 7.1$	$\sigma_1 = 0.107 \cdot z - 30.248$	$\sigma_1 = 0.026 \cdot z + 23.636$
	$\sigma_2 = 0.0193 \cdot z + 4.5$	$\sigma_2 = 0.0715 \cdot z - 20.165$	$\sigma_2 = 0.016 \cdot z + 17.104$
	$\sigma_3 = 1 \times 10^{-6} \cdot \rho \cdot g \cdot z$	$\sigma_3 = 1 \times 10^{-6} \cdot \rho \cdot g \cdot z$	$\sigma_3 = 1 \times 10^{-6} \cdot \rho \cdot g \cdot z$
Rock density ρ (kg/m ³)	2600	2600	2600
Stress orientation	$\sigma_1 - 45/0$ (strike/dip)	$\sigma_1 - 45/0$ (strike/dip)	$\sigma_1 - 45/0$ (strike/dip)
	$\sigma_2 - 135/0$ (strike/dip)	$\sigma_2 - 135/0$ (strike/dip)	$\sigma_2 - 135/0$ (strike/dip)
	$\sigma_3 - 0/90$ (strike/dip)	$\sigma_3 - 0/90$ (strike/dip)	$\sigma_3 - 0/90$ (strike/dip)
Peak UCS (MPa)	40	90	210
Geothermal gradient (°C/m)	0.016	0.016	0.012
Linear thermal expansion (1/°C)	2×10^{-6}	6.7×10^{-6}	10×10^{-6}

2.2 ASSUMPTIONS

Preliminary near-field modelling for the purpose of a DGR design assumes that each of the materials used in the modelling is homogeneous, isotropic, temperature-independent and linearly elastic. The rock mass around the DGR is assumed to be infinite in the horizontal extent. The rock mass is further assumed to be intact. The ice load and the thermal influence of ice during glaciation on the thermal and mechanical response will not be considered in this modelling exercise.

2.3 MATERIAL PROPERTIES

USED FUEL

The heat output from the used fuel from each UFC is shown in Table 2. All of used fuel is assumed to undergo an initial cooling period of 30 years in surface facilities prior to placement within the DGR and the DGR is assumed to be filled instantaneously with 30-year-out-of-reactor fuel at the reference conditions.

ROCK MASS

The in-situ stresses in the sedimentary rock (shale and limestone) and in the granite are shown in Table 1. In this modelling, the in-situ stresses for the shale are extended to the ground surface.

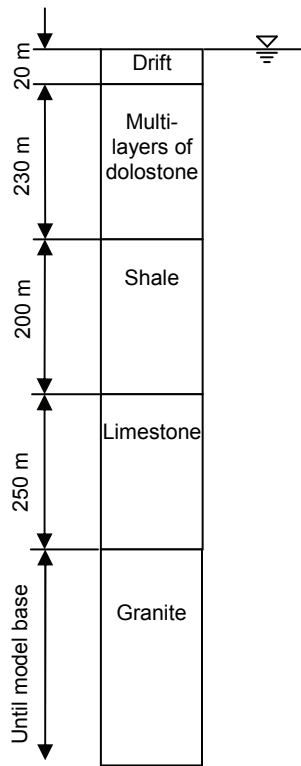


Figure 2: Lithostratigraphic Column – Limestone Geosphere (after SNC-Lavalin (2010)) (drawing not to scale)

The Hoek and Brown empirical failure is adopted to evaluate the stability of the rock mass near the placement tunnel wall and roof. The modified empirical equation of the Hoek and Brown failure criterion is given by:

$$\sigma_{1f} = \sigma_3 + \sigma_{ci} \left(m_b \frac{\sigma_3}{\sigma_{ci}} + s \right)^a \quad (1)$$

where σ_{1f} is the major principal stress at failure;

σ_3 is the minor principal stress;
 σ_{ci} is the uniaxial compressive strength of the intact rock materials from which the rock mass is made up; and
 m_b , s and a are empirical constants.

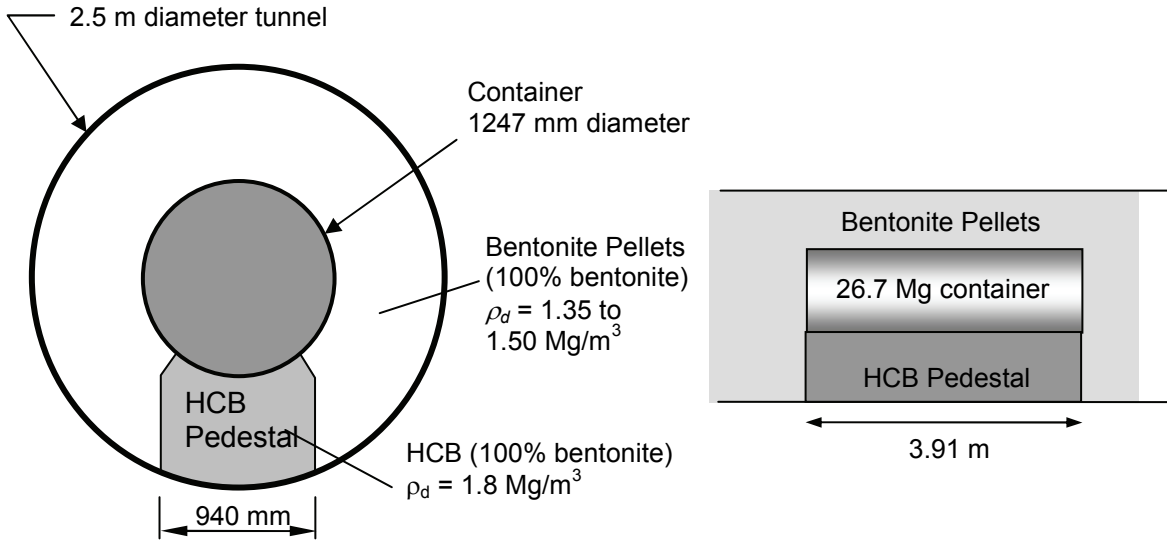


Figure 3: Geometry of the HTP Method

For limestone, the parameters of Eq. 1 are $m_b = 4.1$, $s = 0.0622$ and $a = 0.501$; for shale, the parameters of Eq. 1 are $m_b = 2.3$, $s = 0.0205$ and $a = 0.502$; and for granite, the parameters of Eq. 1 are $m_b = 11.5$, $s = 0.0622$ and $a = 0.501$ (from Golder Associates, personal communication).

The ambient temperature gradient in the rock mass is $0.016^\circ\text{C}/\text{m}$ with a ground surface temperature of 5°C .

SEALING-MATERIALS

The difference of the parameters for the highly compacted bentonite pedestal and bentonite pellets is not considered in this modelling for the purpose of a DGR design. Therefore, both are taken as being a pellet-type bentonite sealing material for the purposes of thermal and mechanical analyses. This is a conservative assumption since the pedestal material is much denser and more thermally conductive than pellets. Their thermal and mechanical parameters are shown in Table 3.

USED-FUEL CONTAINER

The thermal conductivity of the used-fuel container is $300 \text{ W}/(\text{m}^\circ\text{C})$. The density of the used-fuel container is $7800 \text{ kg}/\text{m}^3$. The specific heat of the used-fuel container is $500 \text{ J}/(\text{kg}^\circ\text{C})$. The Young's modulus is $200,000 \text{ MPa}$ and the Poisson's ratio is 0.2 .

Table 2: Heat Output of Containers of Used CANDU Fuel at Different Times

Time Out-of-reactor (years)	Heat Generation (220 MWh/kg U Burn-up)		
	Watts per kg U	Watts per bundle	(W/container) (360 bundles)
30	1.83E-01	3.52	1268.2
35	1.68E-01	3.23	1164.2
40	1.54E-01	2.97	1069.2
45	1.42E-01	2.74	986.4
50	1.32E-01	2.53	910.8
55	1.22E-01	2.35	846.0
60	1.14E-01	2.19	788.4
70	9.91E-02	1.908	686.9
75	9.30E-02	1.791	644.8
80	8.75E-02	1.685	606.6
90	7.82E-02	1.505	541.8
100	7.07E-02	1.361	490.0
110	6.47E-02	1.245	448.2
135	5.41E-02	1.041	374.8
150	4.99E-02	0.96	345.6
160	4.77E-02	0.918	330.5
200	4.19E-02	0.806	290.2
300	3.55E-02	0.684	246.2
500	2.91E-02	0.56	201.6
1,000	2.02E-02	0.388	139.7
2,000	1.38E-02	0.265	95.40
5,000	1.00E-02	0.1926	69.34
10,000	7.19E-03	0.1385	49.86
20,000	4.16E-03	0.0801	28.84
35,000	2.27E-03	0.0437	15.73
50,000	1.43E-03	0.0274	9.864
100,000	4.41E-04	0.00849	3.056
200,000	1.65E-04	0.00317	1.141
250,000	1.52E-04	0.00293	1.055
500,000	1.48E-04	0.00285	1.026
1,000,000	1.48E-04	0.00285	1.026

Table 3: Thermal and Mechanical Properties of the Bentonite Buffer Pellets

Thermal conductivity (W/m°C)	0.4	Specific heat (J/kg°C)	920
Bulk density (kg/m ³)	1410	Dry density (kg/m ³)	1410
Porosity (%)	49	Young's modulus (GPa)	0.1
Poisson's ratio	0.1	Linear thermal expansion (1/°C)	NA

3. NEAR-FIELD MODELLING

In this section, the thermal modelling and coupled T-M modelling are described. The modelling was conducted using CODE_BRIGHT (CODE_BRIGHT_v3beta, which was the latest version at the time of performing this modelling) (Olivella et. al., 1996; CODE_BRIGHT User's Guide, 2009) and GiD (Version 9.0.6) is used in pre-processing and post-processing the input and output data from CODE_BRIGHT.

In order to simplify the near-field model, the parameters of the rock mass in the whole model use the parameters of the limestone. The purpose of near-field modelling is studying the local thermal and mechanical response near the container. Therefore, this simplification will not significantly influence the results for the location response.

3.1 NEAR-FIELD THERMAL MODELLING

3.1.1 Geometry

The finite-element discretization of a unit cell using the HTP method for the near-field modelling of the thermal evolution is shown in Figure 4. There are three kinds of materials: limestone, buffer material and container. The diameter of the placement tunnel is 2.5 m. The dimensions of the container are 3,909 mm long and 1,247 mm in diameter.

The horizontal dimensions of a unit cell are 10 m x 4 m (10 m is half of the placement tunnel spacing and 4 m is the half of the container spacing). The vertical dimension of the model unit cell is 5,000 m. The depth of the crown of the placement tunnel is 500 m. Eight-noded elements are used through the model. The elements are more densely distributed in the region of high thermal and stress gradients as shown in Figure 4. There are 25,284 nodes and 22,200 elements in the near-field thermal model.

3.1.2 Boundary Conditions and Initial Conditions

Thermal boundary conditions for the model are, shown in Figure 4, are as follows:

- The temperature on the top surface (ground surface) is 5°C.
- An isothermal condition is applied at the bottom of the model (i.e., 5,000 m below ground surface) at a temperature of 85°C. The geothermal gradient is 0.016°C/m.

- An adiabatic condition is applied on the four vertical surfaces of the model due to mirror symmetry, which represents the thermal conditions associated with this unit cell within an infinite tabular array of placement tunnels.
- A uniform thermal load is applied at the nodes (12 nodes) along the axis of the container. The total thermal load applied to the 12 nodes is one quarter (1/4) of the container thermal load (Table 1) due to the intersection of two adiabatic planes at the container centreline.

The thermal boundary conditions described above represent the boundary conditions for a unit cell in a horizontally infinite repository. Based on the study in Guo (2007), the results from the near-field model using the above boundary are accurate only for the first 1,000 years for a horizontally finite repository. After 1,000 years, the temperatures calculated will be several degrees in error if the results are used for a horizontally finite repository (Guo 2007).

Initial temperatures in the whole model are calculated from the following equation:

$$T_0 = 5(^{\circ}C) + 0.016(^{\circ}C/m) \cdot z(m) \quad (2)$$

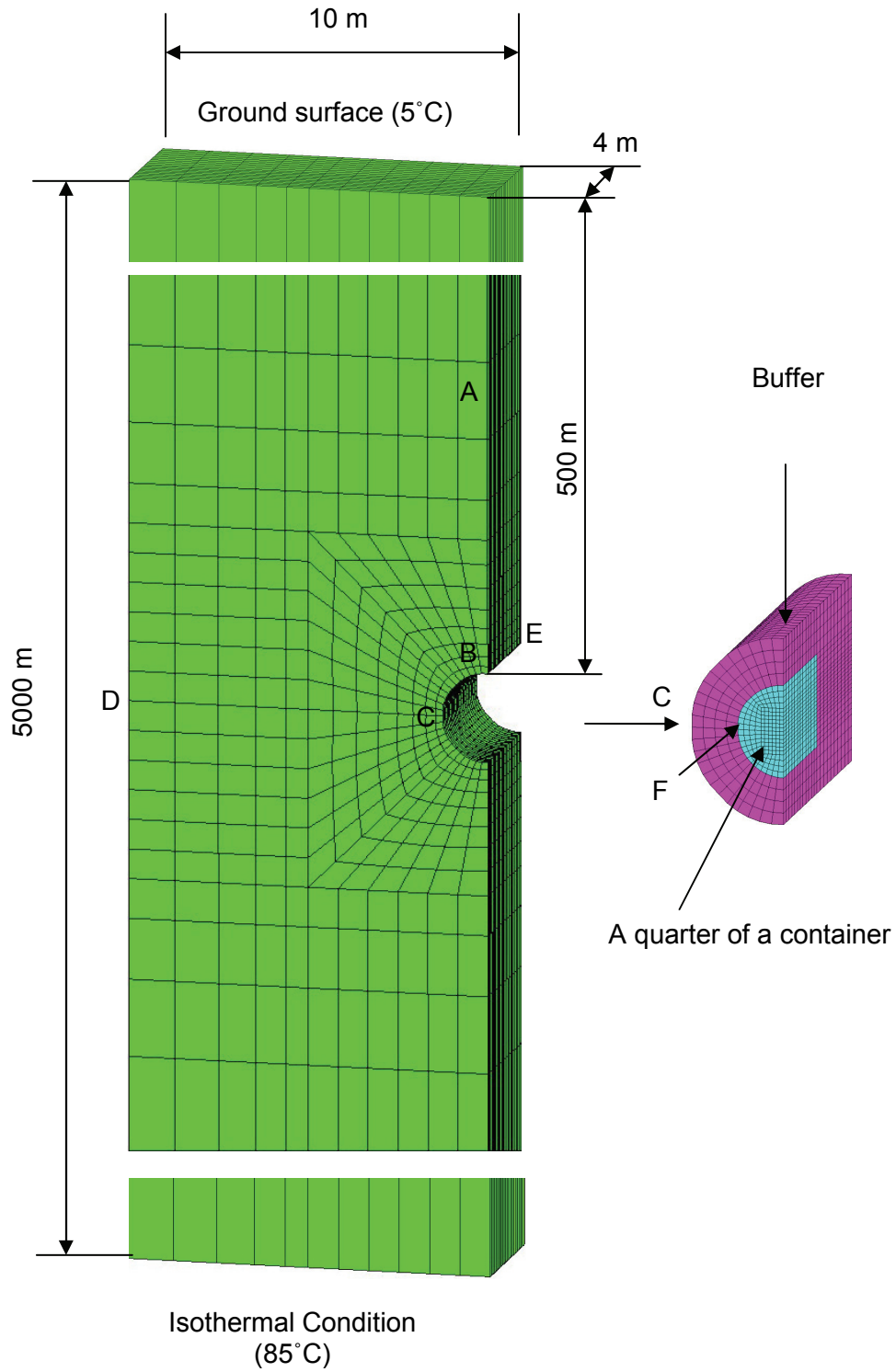


Figure 4: Dimensions and Meshes of the Near-Field Model

3.1.3 Thermal Results from the Near-field Thermal Model

Figure 5 shows the temperature calculated using CODE_BRIGHT at different locations along the horizontal line FCD (see Figure 4 for location). The temperature on the container surface reaches a peak of 117.4°C at 10 years of waste placement. On the surface of the tunnel, the peak temperature is 69.0°C and 72.0°C at 50 years and 1,000 years after placement, respectively.

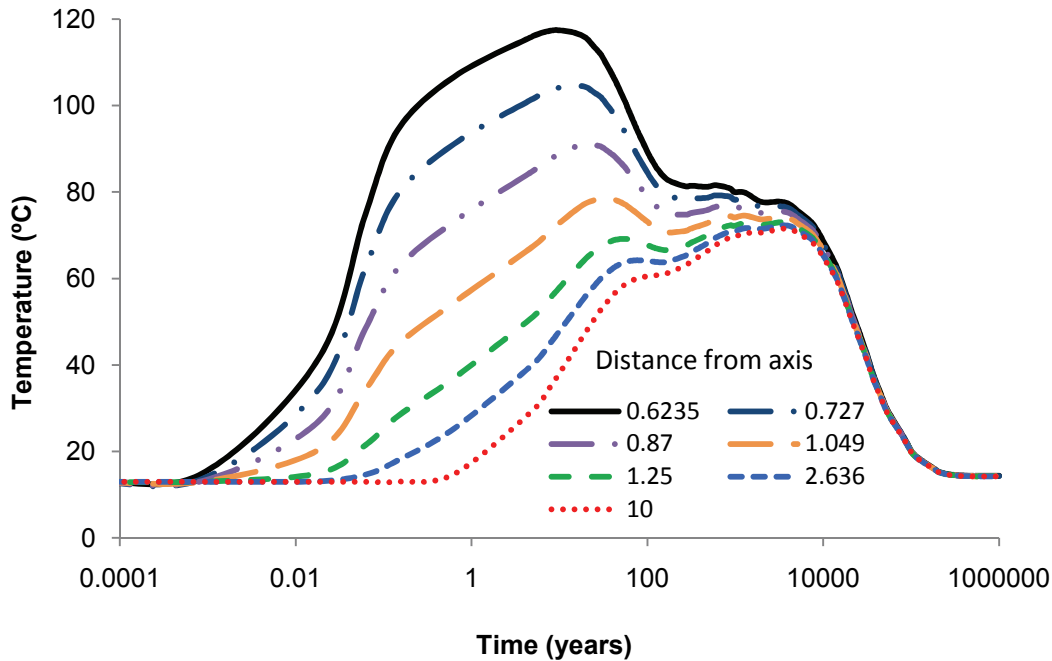


Figure 5: Temperatures at Different Locations along Horizontal Line FCD (see Figure 4 for the location of this line)

Figure 6 shows the temperature versus the distance from the tunnel axis along the horizontal line FCD at different times. After 1,000 years of placement, the temperature in the rock is very uniform at a value of ~72.0°C.

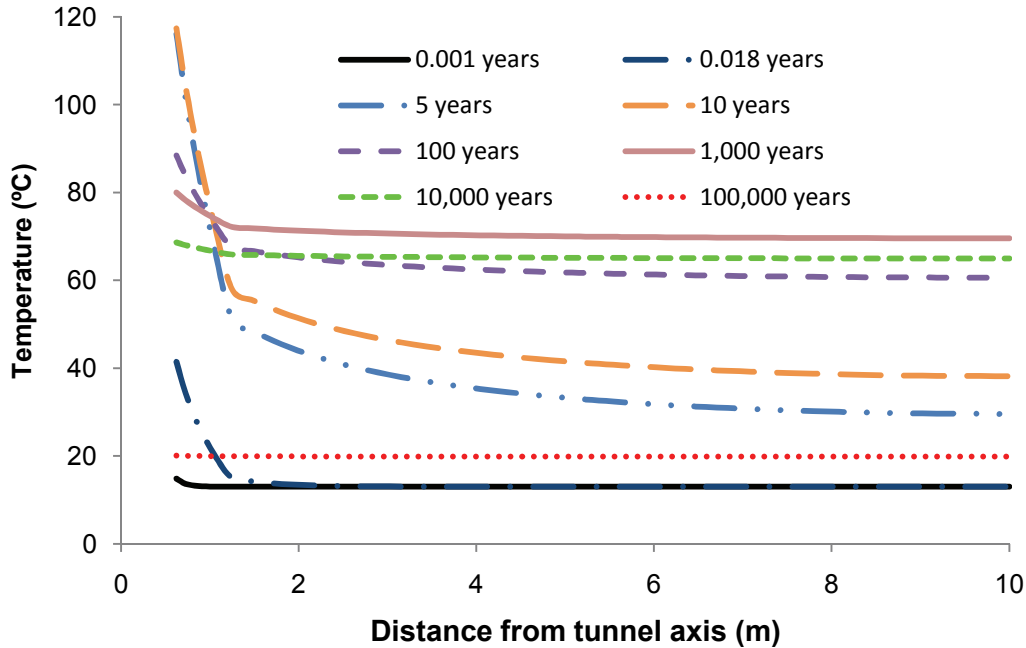


Figure 6: Temperatures along Horizontal Line FCD (see Figure 4 for location) at Seven Different Times

Figure 7 shows the temperature versus time at different locations along the vertical line BA. Figure 8 shows the temperature versus the distance from the tunnel axis along vertical line BA. Since Figures 5 and 78 show a similar trend, one can assume that the temperatures around the container are axisymmetric along the horizontal axis.

Figure 9 shows the temperatures versus time at four different locations along the tunnel roof (line BE in Figure 4). The first peak temperatures are from 69.0°C to 64.0°C at 50 to 80 years after placement at different locations. The second peak temperatures are at 72.0°C at about 1,000 years after placement at different locations along the tunnel roof. Figure 10 shows the temperature versus horizontal distance from the container centre along the tunnel roof. Except for 5 years after placement, the temperatures are very uniform along the tunnel roof.

Figures 11 and 12 show the temperature contours in the rock surrounding the buffer and in the buffer at four different times.

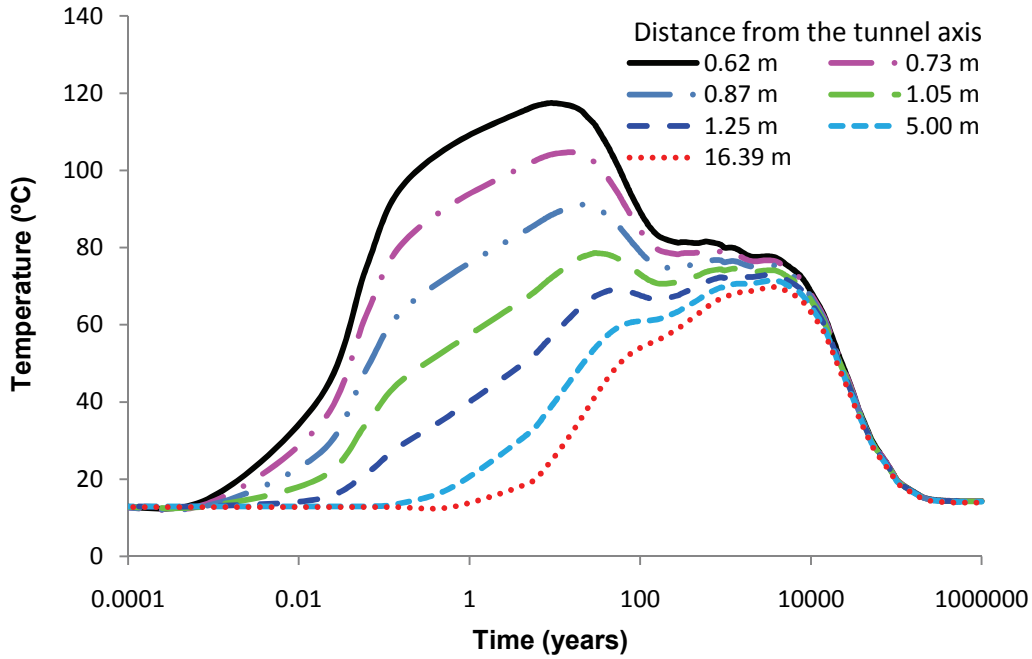


Figure 7: Temperatures at Different Locations along Vertical Line BA (see Figure 4 for the location of this line)

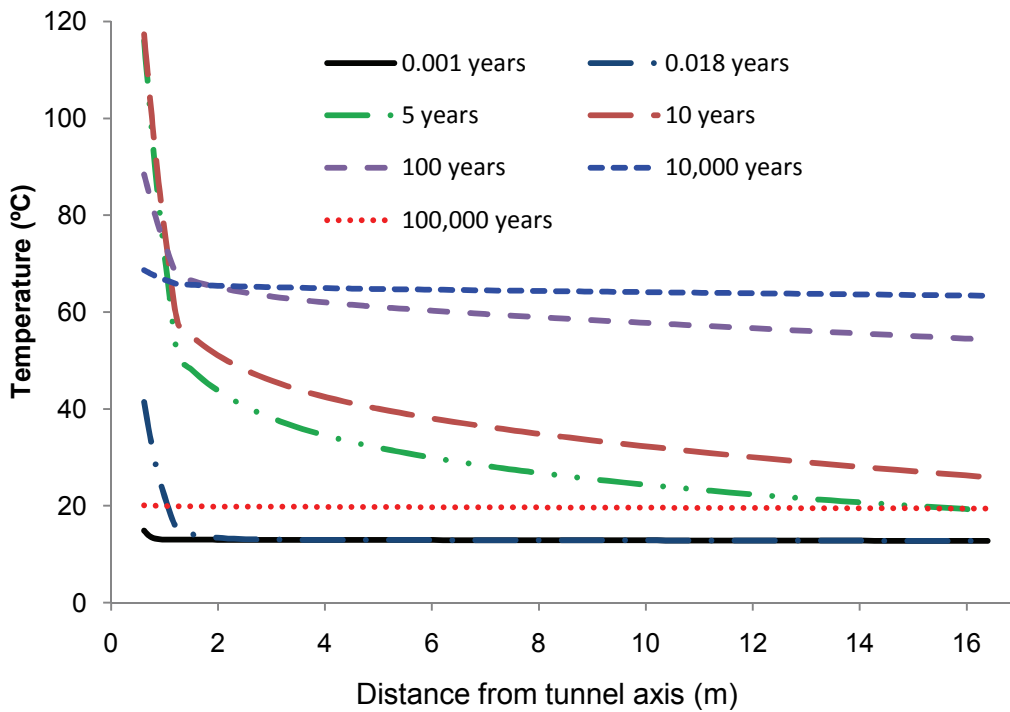


Figure 8: Temperatures along Vertical Line BA at Seven Different Times (see Figure 4 for the location of this line)

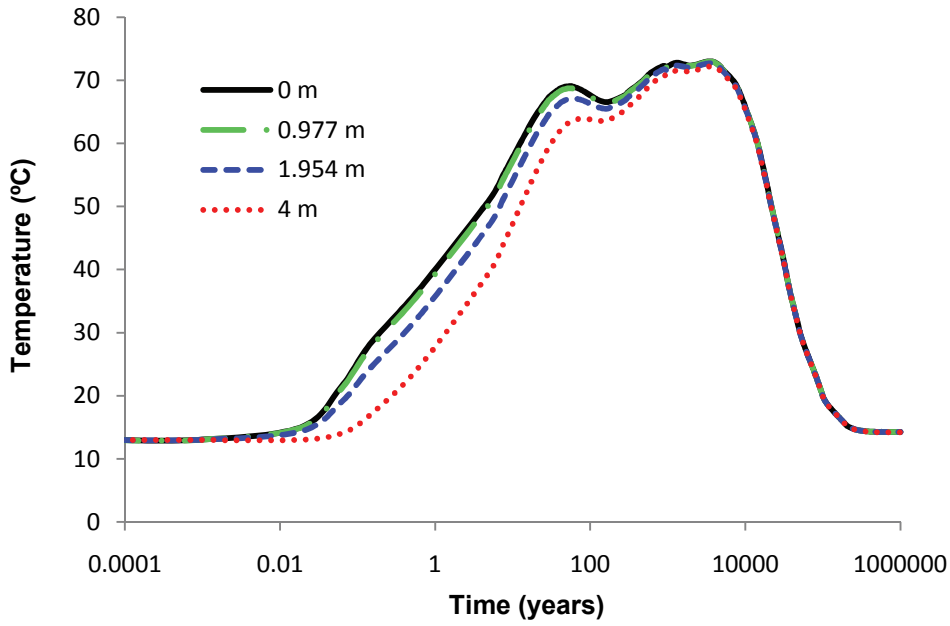


Figure 9: Temperatures at Four Locations along Tunnel Roof BE (see Figure 4 for the location of the line of BE)

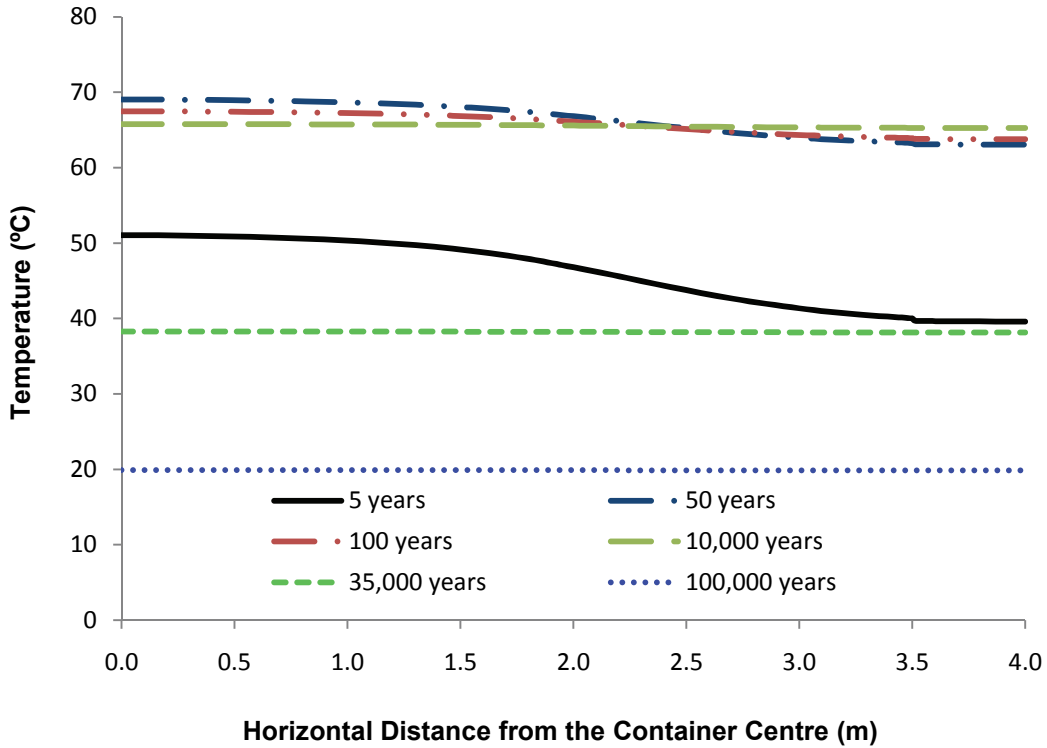


Figure 10: Temperature along Tunnel Roof BE at Six Different Times

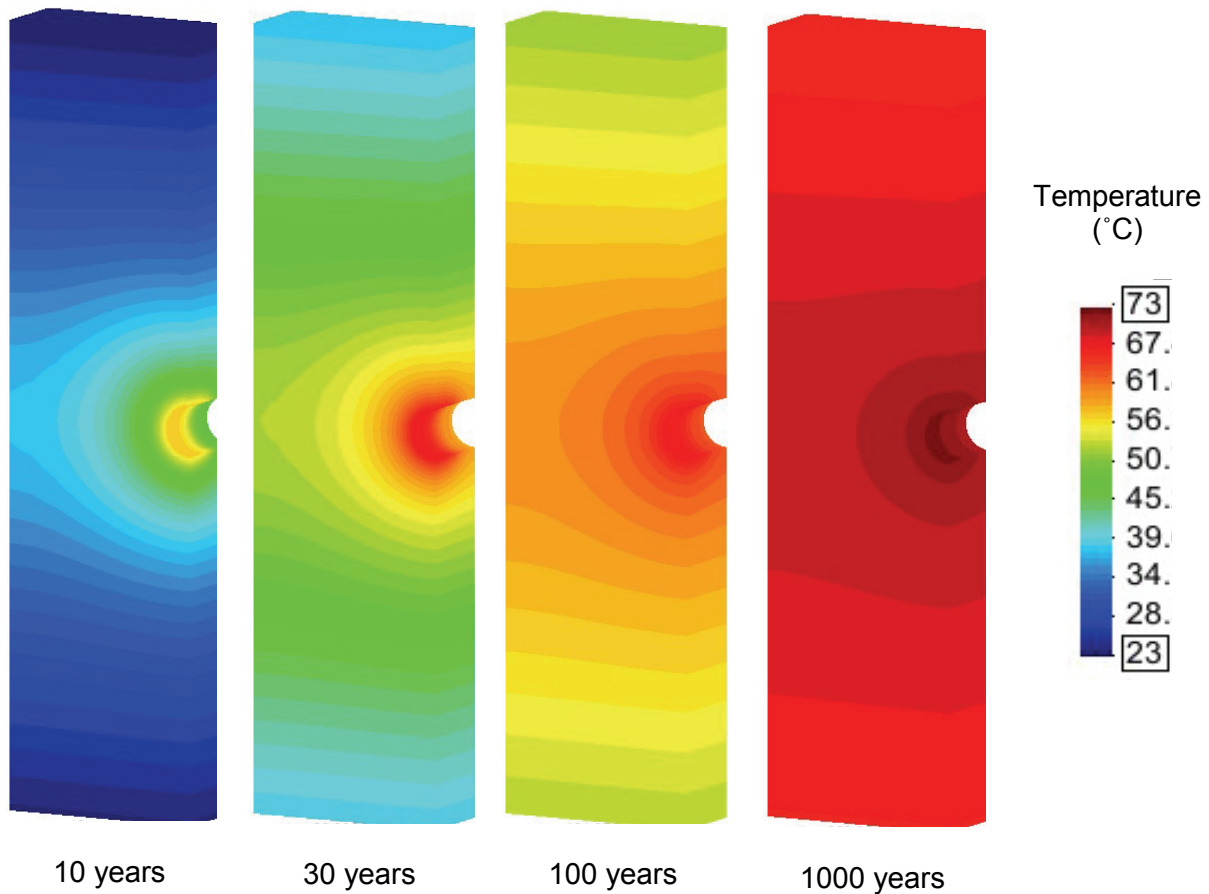


Figure 11: Temperature Contours in the Rock surrounding the Buffer

3.2 Near-Field Coupled T-M Modelling

In order to understand the influence of the used fuel released thermal load in a DGR on the local mechanical stability around the placement tunnel, a coupled T-M model is described in this section.

3.2.1 Model Geometry, Boundary Conditions and Initial Conditions

MODEL GEOMETRY

Using Figure 4 as the geometry for the coupled T-M near-field model proved problematic and the calculation will not converge due to large aspect ratio for some elements near the top and near the bottom of the model shown in Figure 4. Therefore, only part of Figure 4 is used as the coupled T-M near-field model geometry, as shown in Figure 13. The horizontal dimensions are the same as the thermal-only model (10 m by 4 m), but the vertical dimension is reduced to 200 m versus 5,000 m used in the thermal calculation. In this case, the top and the bottom of the model locate at a depth of 400 m and 600 m, respectively in the limestone. As mentioned before, the near-field modelling is studying the local mechanical response, there will not be

significant difference consequent of the results using the model as shown in Figure 13 if the suitable boundary conditions are applied.

Within the adjusted T-M repository model there are 22,260 nodes and 22,484 eight-noded elements present.

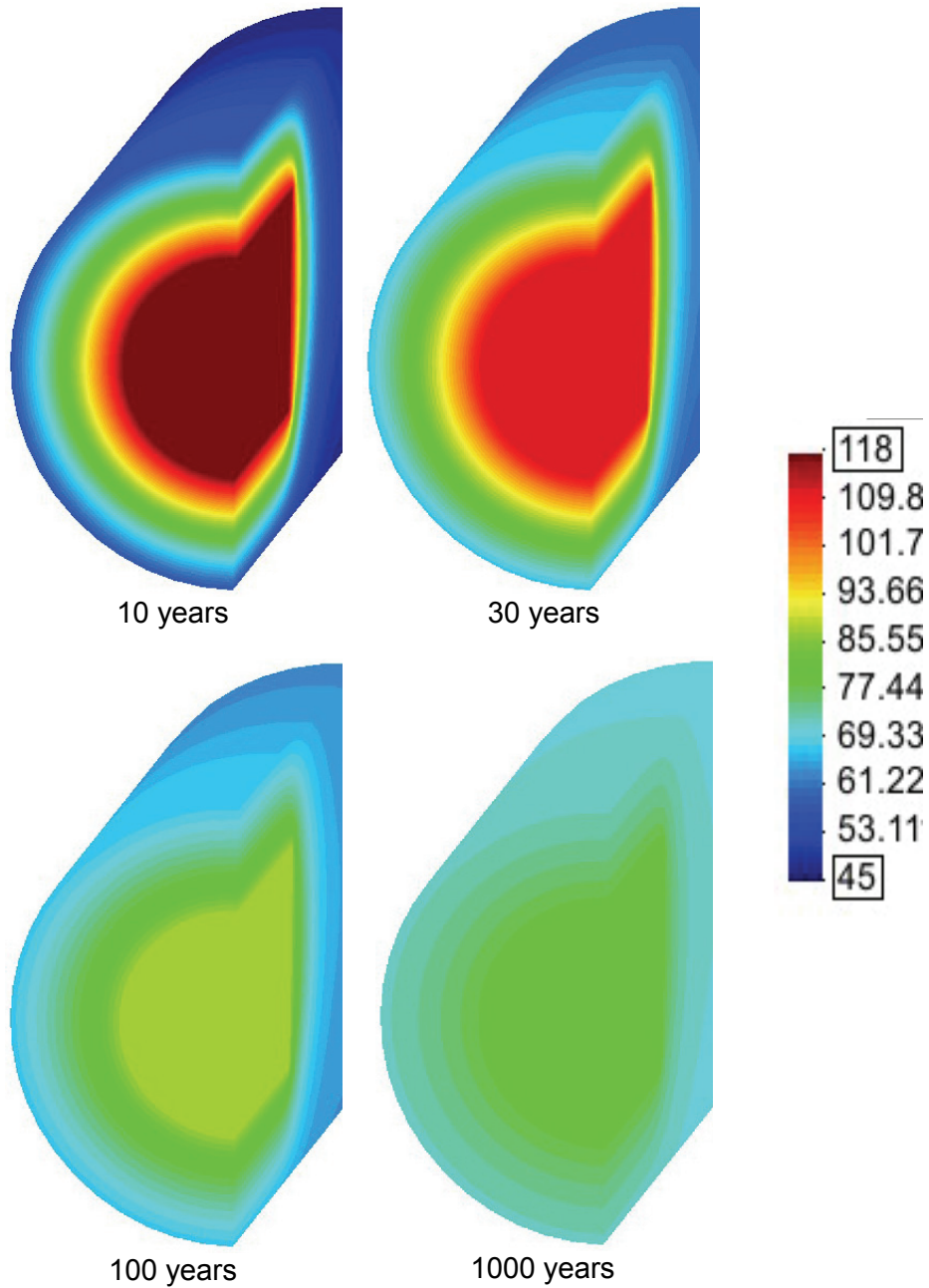


Figure 12: Temperature Contours in the Buffer at Four Different Times

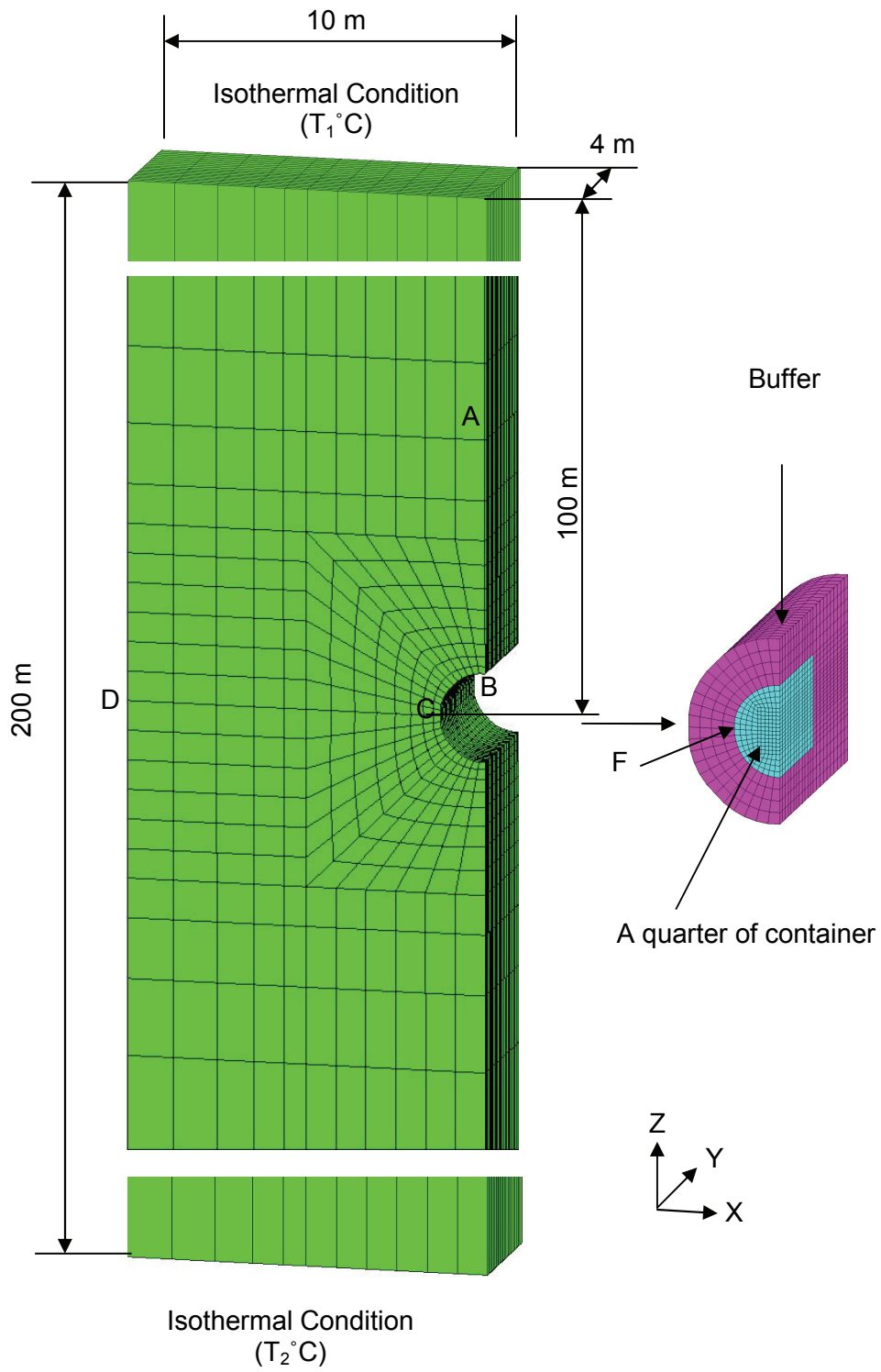


Figure 13: Geometry and Meshes for the Coupled T-M Near-field Model

THERMAL BOUNDARY CONDITIONS

As noted above, the T-M analysis required a change in the original model geometry in order to obtain convergence in the calculations. In order to model the resultant smaller volume in the T-M calculations there were some changes in the boundary conditions that were required to simulate the conditions that would develop at a 500 m depth. These thermal values and conditions were as follows.

- The temperatures on the top and the bottom of the T-M model are T1 and T2, respectively, as shown in Figure 14, and are the results calculated from the thermal-only model at the same locations as shown in Section 3.1.
- An adiabatic condition is applied on the four vertical surfaces of the model due to mirror symmetry, which represents the thermal conditions associated with this unit cell within an infinite tabular array of placement tunnels.
- A uniform thermal load is applied at the nodes (12 nodes) along the axis of the container. The total thermal load applied to the 12 nodes is one quarter of a container thermal load.

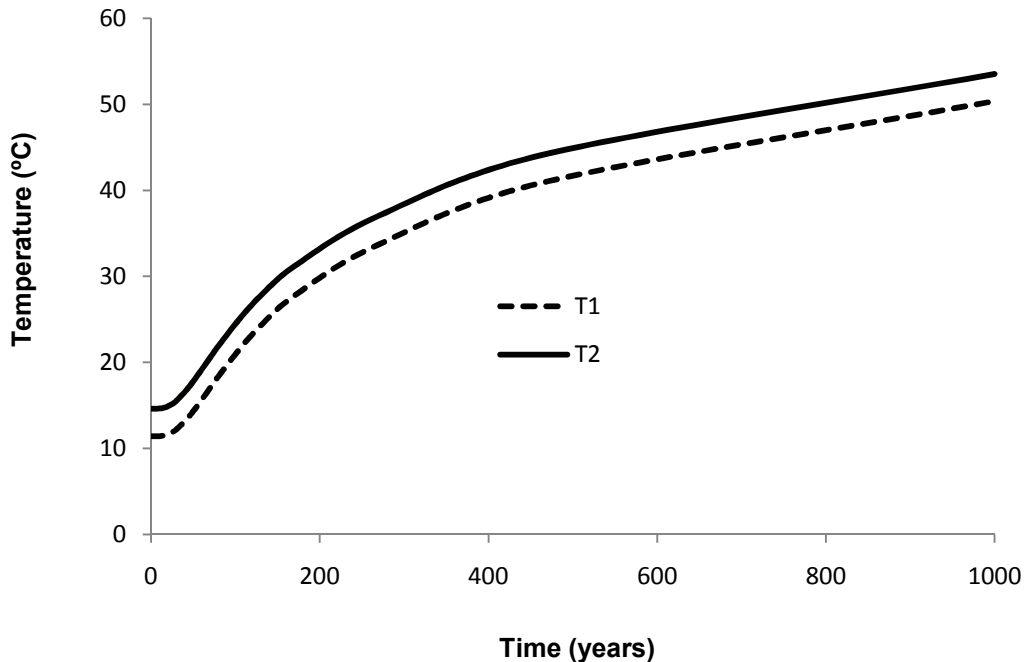


Figure 14: Thermal Boundary Conditions of the Coupled T-M Model

MECHANICAL BOUNDARY CONDITIONS

- The vertical planes of the model are constrained not to move in the horizontal direction.
- The bottom plane of the model is fixed in the vertical direction.
- A compressive surface stress of 13.0 MPa, which is the initial vertical stress in the rock on the repository level, is applied on the top surface of the model.

INITIAL THERMAL AND MECHANICAL CONDITIONS

- The initial temperatures in the model are as follows: the geothermal gradient is 0.016°C/m of depth; the top of the model temperature is 11.4°C and the model bottom temperature is 14.6°C.
- The initial stresses in the rock are 15.6 MPa, 23.3 MPa and 13.0 MPa in the X-, Y-, and Z-directions, respectively, which are the in situ stresses at the repository depth of 500 m in limestone (see Table 1). In this model, the variation of stresses with depth is not considered.
- The initial stresses in the buffer and the container are set at 0 MPa in the X-, Y-, and Z-directions.

Due to the symmetry of the model, the stresses in the X-, Y-, and Z-directions are the major stresses in this model.

3.2.2 Thermal Results from the Coupled T-M Model

Figure 15 shows the comparison of temperatures versus time at three different locations along the horizontal line FCD. The temperatures from the coupled T-M model matched the temperatures from thermal-only model very well for all locations. This provides confidence that the adjustments and revised boundary conditions necessary to conduct the coupled T-M near-field analyses were appropriate.

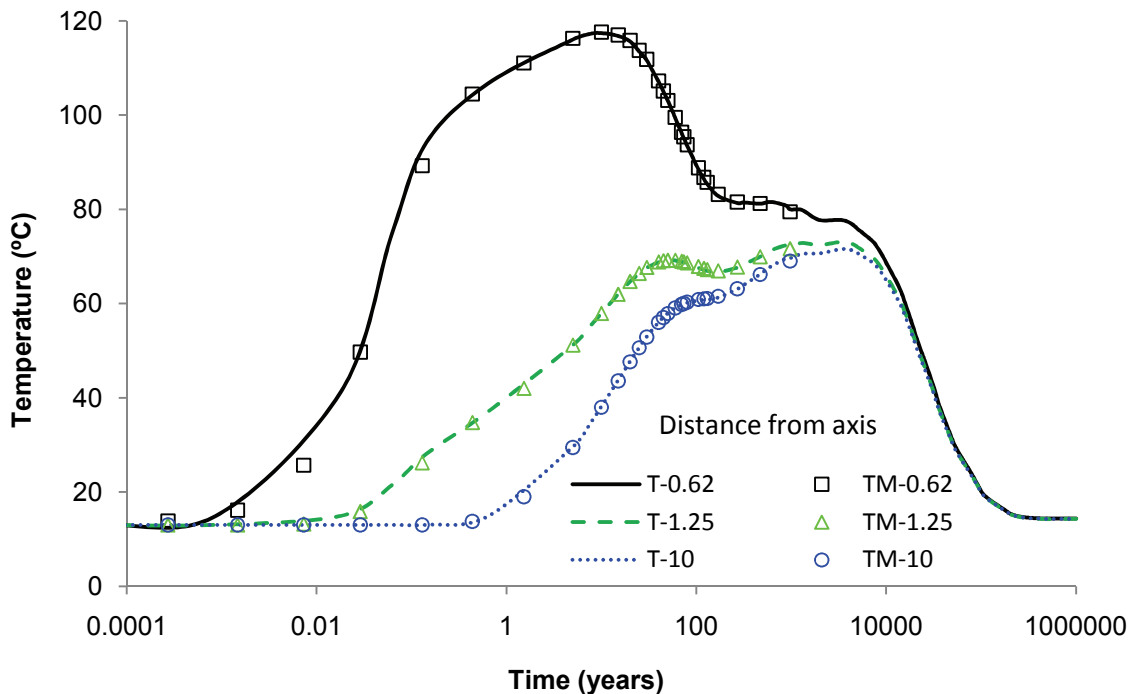


Figure 15: Comparison of Temperature at Three Different Locations along Horizontal Line FCD between Thermal Only Model (T-) and Coupled T-M Model (TM-)

3.2.3 Mechanical Results from the Coupled T-M Model

Figure 16 shows the X-directional stresses along the vertical line BA above the tunnel roof. The excavation-induced X-directional stresses at 0 years (i.e., before UFC placement) are 28.9 MPa at 0.1 m from the roof surface and 15.7 MPa at 7.65 m from the tunnel roof surface. The total stresses including thermally induced and excavation-induced stresses, are 66.4 MPa at 0.1 m from the roof surface and 31.0 MPa at 7.65 m from the tunnel roof surface after 1,000 years of placement.

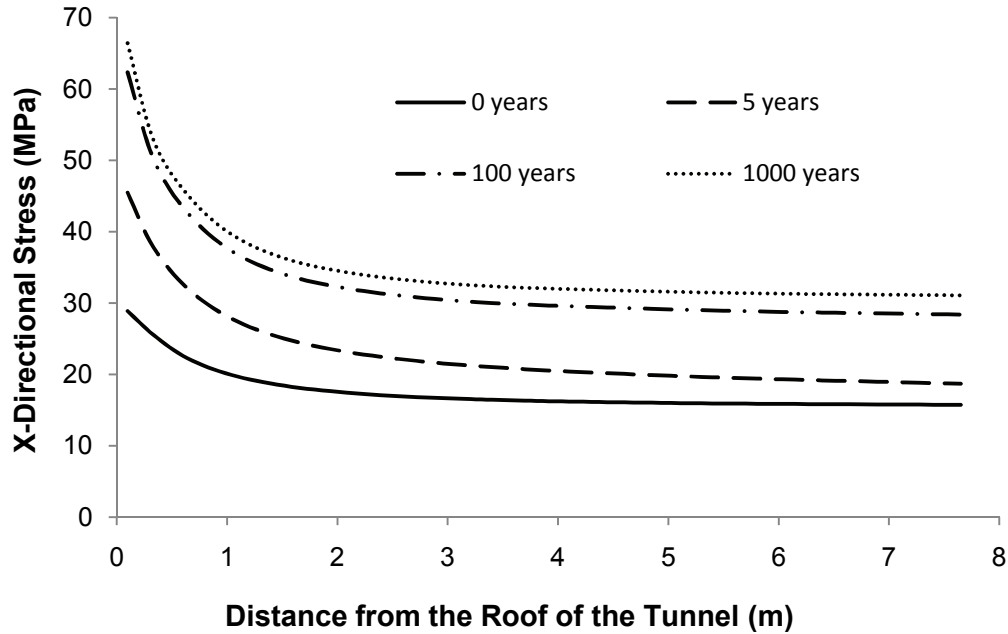


Figure 16: X-Directional Stresses along Vertical Line BA

Figure 17 shows the Y-directional stress versus distance from the tunnel roof along the vertical line BA above the tunnel roof. The excavation-induced Y-directional stresses at 0 years (i.e., before UFC placement) are 23.9 MPa (initial stress value is 23.3 MPa) at 0.1 m from roof surface and 23.3 MPa at 7.65 m from the tunnel roof surface. The total Y-directional stresses are 47.0 MPa at 0.1 m from the tunnel roof surface and 38.0 MPa at 7.65 m from the tunnel roof surface after 1,000 years of placement.

Figure 18 shows the Z-directional stresses versus distance from the tunnel roof along the vertical line BA above the tunnel roof. The excavation-induced Z-directional stresses at 0 years (i.e., before UFC placement) are 1.9 MPa at 0.1 m from roof surface, 11.0 MPa at 1.5 m from the roof surface and 12.9 MPa at 7.65 m from the tunnel roof surface, respectively. The total stresses including excavation-induced and thermally induced Z-directional stresses are 3.2 MPa at 0.1 m from the tunnel roof surface, 14.7 MPa at 1.5 m from the roof surface and 13.4 MPa at 7.65 m from the tunnel roof surface after 1,000 years of placement.

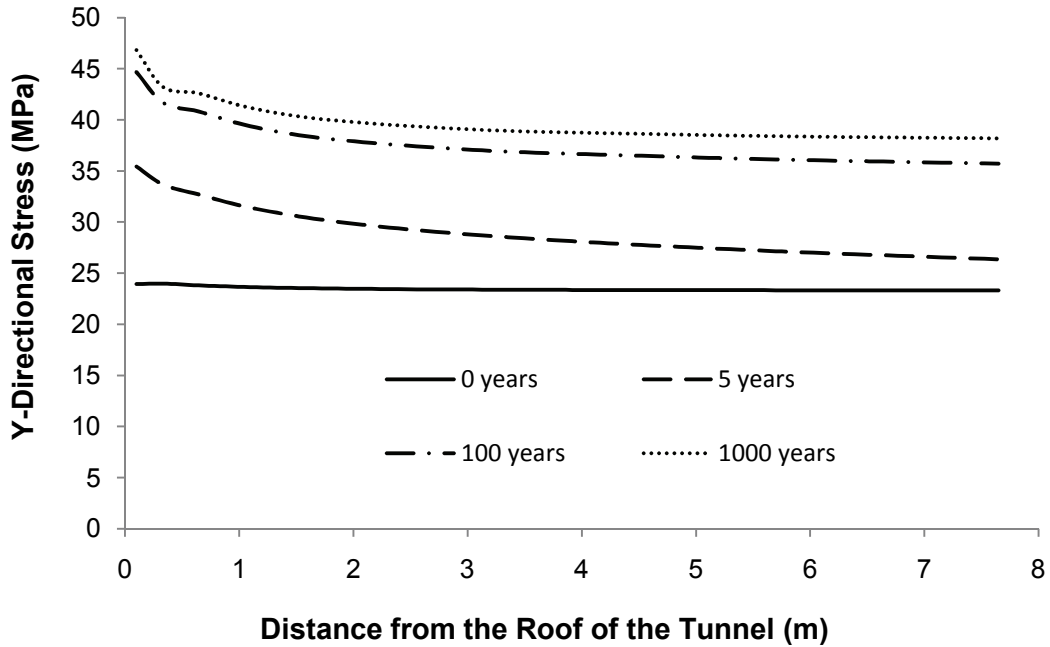


Figure 17: Y-Directional Stresses along Vertical Line BA

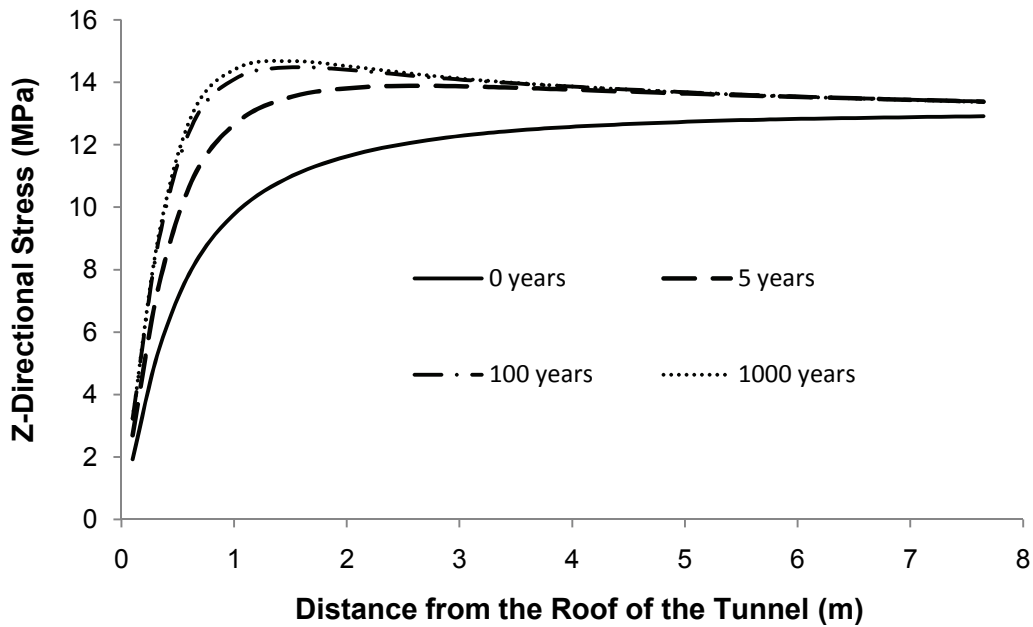


Figure 18: Z-Directional Stresses along Vertical Line BA

Figure 19 shows the X-directional stresses versus distance from the tunnel wall along the horizontal line CD. Excavation-induced X-directional stresses at 0 years (i.e., before UFC placement) are 1.6 MPa at 0.1 m from the tunnel wall and 14.9 MPa at 8.1 m from the tunnel

wall. The total stresses including excavation-induced stresses and thermal stresses are 1.4 MPa at 0.1 m from the tunnel wall and 29.1 MPa at 8.1 m from the tunnel wall after 1,000 years of placement.

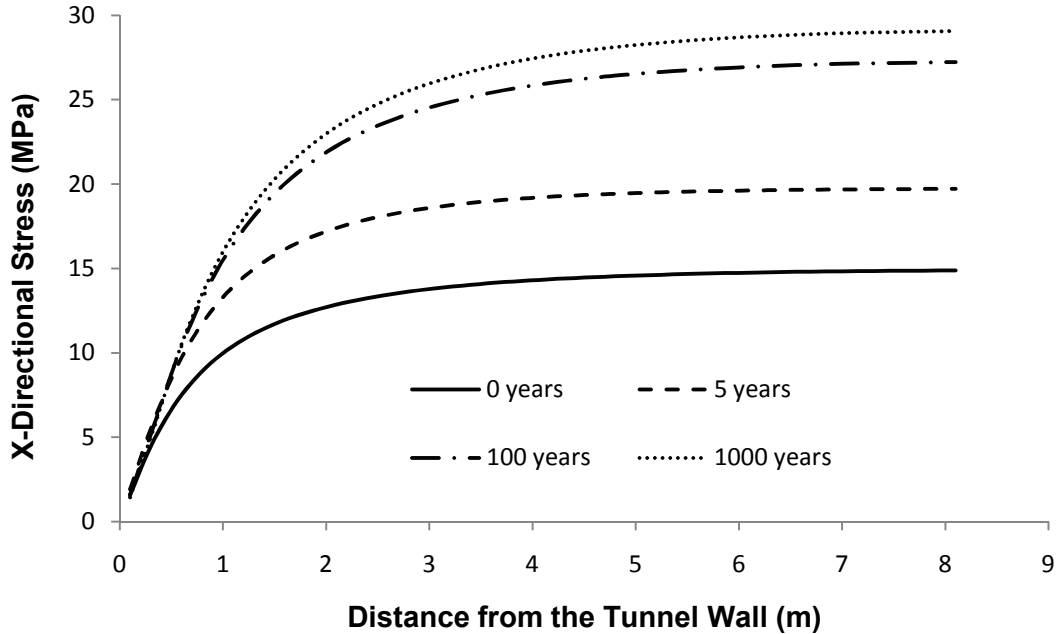


Figure 19: X-Directional Stress along Horizontal Line CD

Figure 20 shows the excavation-induced Y-directional stresses at 0 years (i.e., before UFC placement) and total Y-directional stresses versus distance from the tunnel wall along the horizontal line CD at different times. Excavation-induced Y-directional stresses are 21.8 MPa at 0.1 m from the tunnel wall and 23.2 MPa at 8.1 m from the tunnel wall. The total Y-directional stresses including excavation-induced stresses and thermally induced stresses are 31.0 MPa at 0.1 m from the tunnel surface and 38.0 MPa at 8.1 m from the tunnel wall after 1,000 years of placement.

Figure 21 shows the Z-directional stresses versus distance from the tunnel wall along the horizontal line CD at different times. Excavation-induced Z-directional stresses at 0 years (i.e., before UFC placement) are 22.1 MPa at 0.1 m from the tunnel wall and 13.6 MPa at 8.1 m from the tunnel wall. The total Z-directional stresses including excavation-induced stresses and thermally induced stresses are 24.2 MPa at 0.1 m from the tunnel surface and 12.8 MPa at 8.1 m from the tunnel surface after 5 years of placement. The total Z-directional stresses are 13.2 MPa at 0.1 m from the tunnel surface, 18 MPa at 0.645 m from the tunnel surface and 13.7 MPa at 8.1 m from the tunnel surface after 1,000 years of placement.

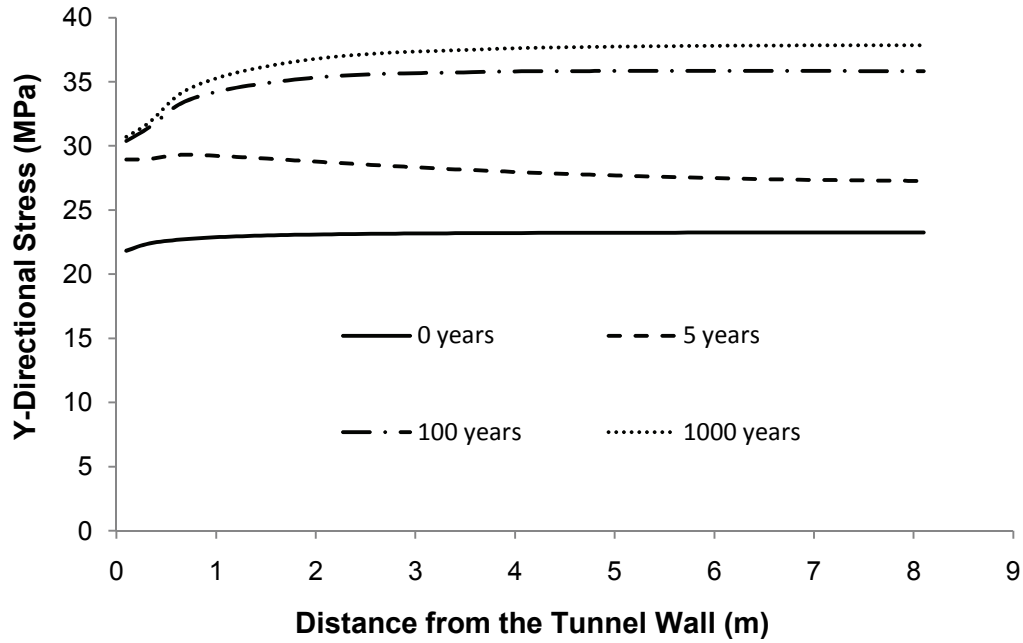


Figure 20: Y-Directional Stress along Horizontal Line CD

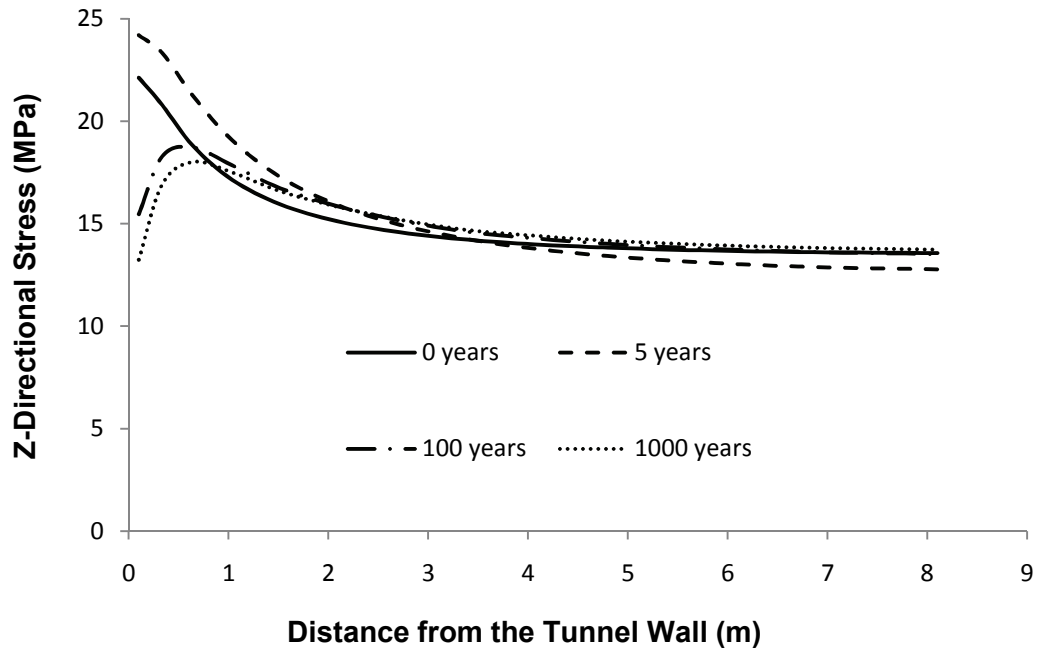


Figure 21: Z-Directional Stress along Horizontal Line CD

3.2.4 Stability Analyses

One means of evaluating the stability of rock around placement tunnel is calculating the factor of safety. Factor of safety is defined as the ratio of the major principal stress at failure to the major principal stress of the rock. In this report it is assumed that a safety factor of less than 1 indicates that the rock is damaged. The safety factor is calculated using the following equation:

$$SF = \frac{\sigma_{1f}}{\sigma_1} \tag{3}$$

in which SF is the safety factor;

σ_{1f} is the major principal stress at failure, MPa, which can be calculated using Eq. (1);

and

σ_1 is the major principal stress, MPa.

Figure 22 shows the safety factors along the vertical line BA. The safety factors are 0.67 at tunnel roof, 1.28 at 0.1 m from the tunnel roof and gradually increase to 3.56 at 2.7 m from the tunnel roof immediately after excavation (i.e., at 0 years and before UFC placement). A damage zone with a thickness 0.053 m will be present at the tunnel roof immediately after excavation.

The safety factors decrease to 0.40 at the tunnel roof and 0.67 at 0.1 m from the tunnel roof and 2.30 at 2.7 m from the tunnel roof after 1,000 years of placement. There is a damage zone with a thickness of 0.211 m after 1,000 years of placement.

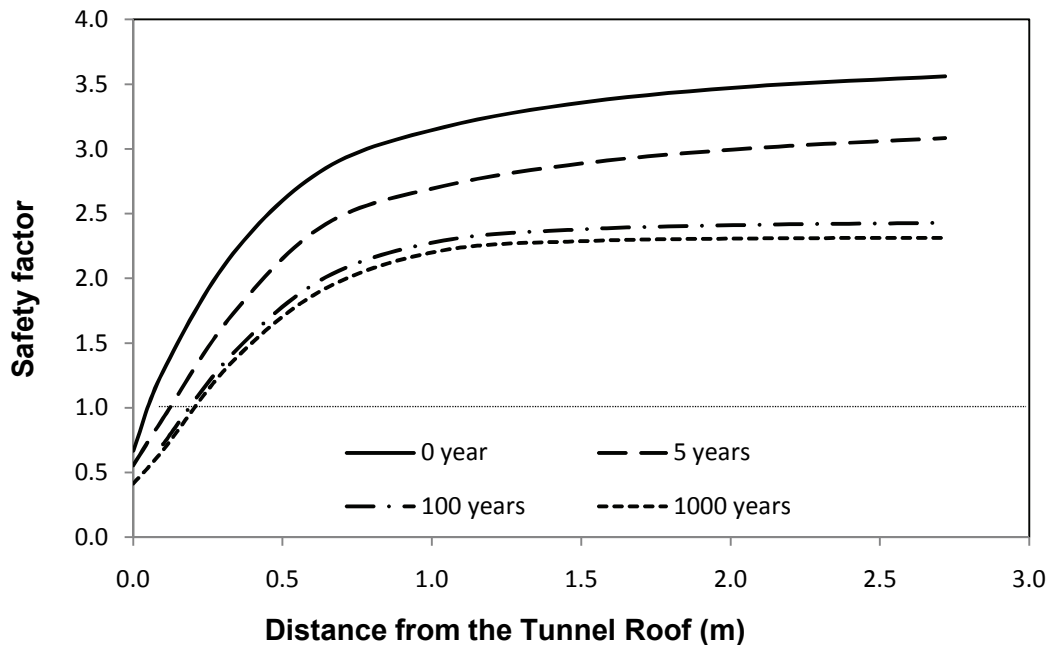


Figure 22: Safety Factors along Vertical Line BA

Figure 23 shows the safety factors along the horizontal line CD at different times. The safety factors are 1.00 at the tunnel wall and 3.80 at 2.7 m from the tunnel wall immediately after

tunnel excavation (i.e., at 0 years and before UFC placement). The safety factors are 0.65 at the tunnel wall, 1.06 at 0.1 m from the tunnel wall and 3.40 at 2.7 m from the tunnel wall after 1,000 years of placement. There is a damage zone with a thickness of 0.077 m after 1,000 years of placement.

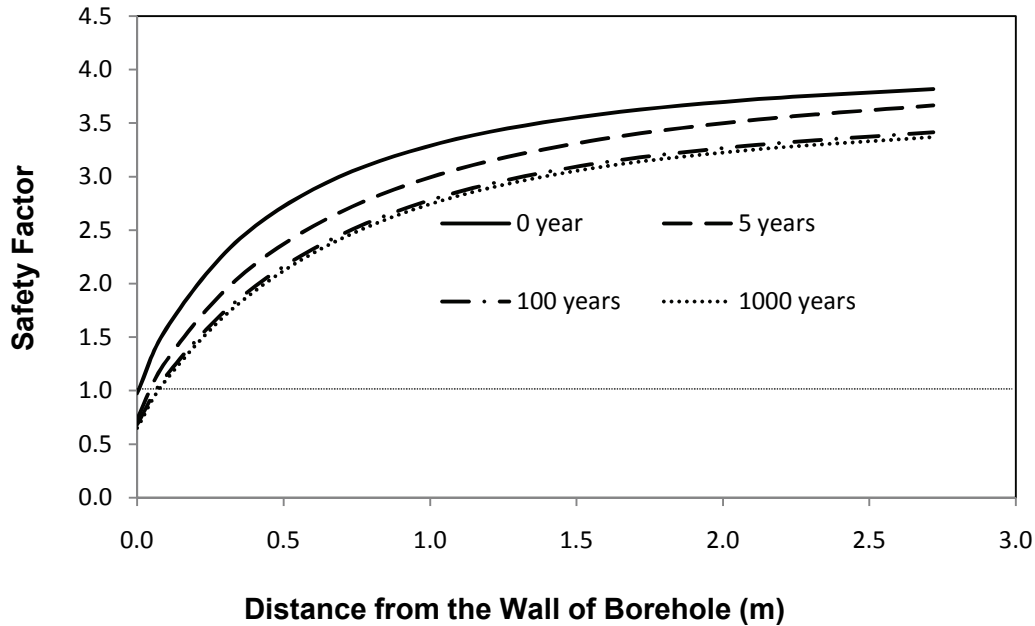


Figure 23: Safety Factors along Horizontal Line CD

In this modelling exercise, it is assumed that there will be no mechanical support of the tunnel wall from the bentonite buffer since it is expected that the saturation process will likely take thousands of years in a DGR in limestone. Based on this assumption, the magnitude of the estimated rock damage zone from the coupled T-M model is considered to be conservative since the swelling pressure from saturated bentonite pellet and pedestal will further reduce the magnitude of the currently estimated rock damage on the tunnel wall. .

3.2.5 Summary of the Results from Near-field Coupled T-M Model

Based on the near-field modelling, the peak temperature of the container surface is 117°C at 10 years after used fuel placement and the peak temperature of the tunnel surface is 69°C at 50 years after used fuel placement.

On the roof of the tunnel, there is a damage zone with a thickness of 0.053 m immediately after tunnel excavation. There is a damage zone with a thickness of 0.211 m in the rock above the tunnel roof after 1,000 years of used nuclear fuel placement. There is no damage zone on the wall immediately after tunnel excavation. After 1,000 years of used nuclear fuel placement, there will be a damage zone with a thickness of 0.077 m.

4. FAR-FIELD MODELLING

This section describes the far-field modelling for a HTP repository with a placement tunnel spacing of 20 m and a centre-to-centre container spacing of 8 m. The plan area of the repository is 2,069 m by 1,455 m and the depth of the repository is fixed at 500 m to the crown of the placement tunnel as shown in Figure 1.

4.1 FAR-FIELD MODEL GEOMETRY, BOUNDARY CONDITIONS AND INITIAL CONDITIONS

The far-field analyses presented in this section provide an assessment of the thermal and stress conditions in the rock mass surrounding a repository of finite dimensions. Uplift of the rock mass due to thermal expansion effects may be important with respect to the physical integrity of the geosphere surrounding the repository and hence to the movement of contaminants. Thermally induced deformation of the site can be estimated including the potential for near-surface fracturing or opening of pre-existing near-surface fractures.

4.1.1 Far-Field Model Geometry and Material Parameters

FAR-FIELD MODEL GEOMETRY

An isometric view of the far-field model of a repository using the HTP method is shown in Figure 24. Due to symmetry, only a quarter section of a DGR needs to be modelled. The model is bounded vertically by the ground surface and by a plane at 10,000 m depth. The horizontal dimensions of the model in the X- and Y-directions are 5,000 m x 5,000 m. These dimensions should be sufficient such that the T-M response of the rock at the boundaries remains unaffected by the presence of the DGR during the simulation time period. The DGR is represented by a 2.5-m-thick plate of horizontal dimensions of a quarter of a DGR are 1034.5 m x 727.5 m.

MATERIAL PARAMETERS

In the far-field model, there are three kinds of rock representing four layers.

- From the ground surface to a depth of 250 m, there are several layers of Dolostone and a 20 m of drift (Figure 2) (The thermal and mechanical parameters of limestone are used for this layer).
- From a depth of 250 m to a depth of 450 m, it is a layer of shale (Figure 2).
- From a depth of 450 m to a depth of 700 m, it is a layer of limestone (Figure 2).
- From a depth of 700 m to a model bottom, it is granite (Figure 2).

The thermal and mechanical parameters for the shale, limestone and granite are provided in Table 1. The shale stress regime is extended through to the ground surface in the far-field modelling. Therefore, the stresses at the ground surface are $\sigma_1=7.1$ MPa of compressive stress, $\sigma_2=4.5$ MPa of compressive stress and $\sigma_3=0$ MPa.

If different values of the thermal conductivity are used for the different layers (shale, limestone and granite), the thermal gradient in the rock mass will not be the constant 0.016 °C/m noted in Table 1. It will have different values for different rocks. Therefore, in order to keep consistency with the near-field model for the initial temperature of 13°C at repository level and 5°C on the

4.1.2 Far-field Model Boundary Conditions and Initial Conditions

4.1.2.1 Thermal Boundary Conditions of the Far-Field Model

The thermal boundary conditions are defined as follows (Figure 25).

- The upper and the bottom surface boundary conditions are modelled as isothermal boundaries, at temperatures of 5°C and 126°C, respectively.
- The vertical boundaries are modelled as adiabatic planes of symmetry as shown in Figure 25.
- The heat generated from the used-fuel containers in one quarter of a repository is uniformly distributed throughout one-quarter of the repository (i.e., a rectangular plate of 1034.5 m long by 727.5 m wide by 2.5 m high (2.5 m is the height of the diameter of the placement tunnel)). The heat is applied at the nodes located in one-quarter of the repository.

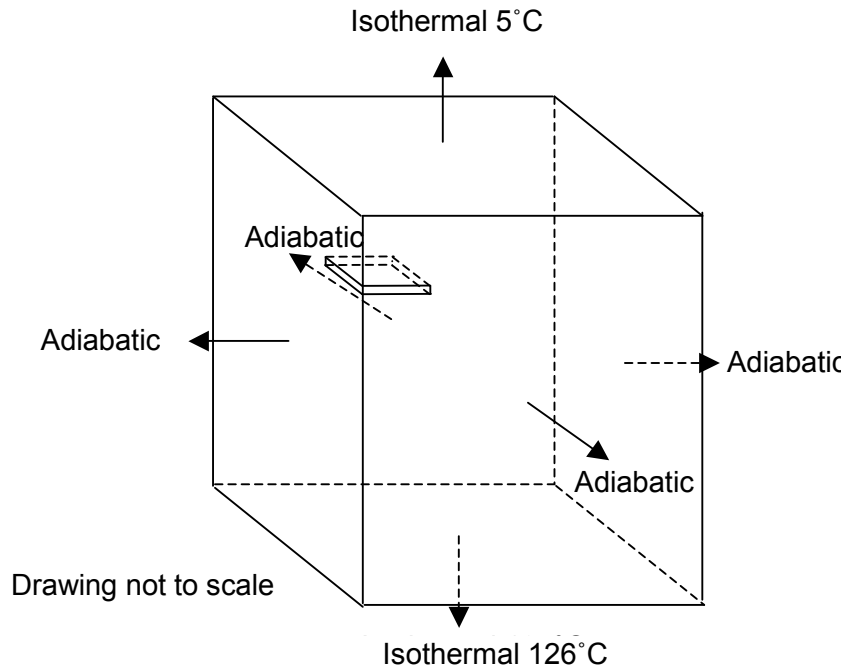


Figure 25: Thermal Boundary Conditions for Far-Field Coupled T-M Model

4.1.2.2 Mechanical Boundary Conditions of the Far-Field Model

The mechanical boundary conditions are defined as follows (Figure 26).

- The vertical planes of the model are constrained so they do not move in the horizontal normal direction.
- The bottom plane of the model is fixed in the vertical direction.
- The upper horizontal plane, the ground surface, is free to move.

4.1.4 Finite Element Discretization

The finite-element discretization of the far-field model is shown in Figure 27. For the purpose of quality assurance, two kinds of meshing were tried and their results are the same. The domain is discretized such that the elements are more densely distributed in the rock mass just above and beneath the repository level where the thermal and mechanical gradients are expected to be the greatest. Dimensions of a typical element within the repository are 36.375 m x 41.38 m x 1.25 m. The number of the elements and nodes is shown in Figure 27.

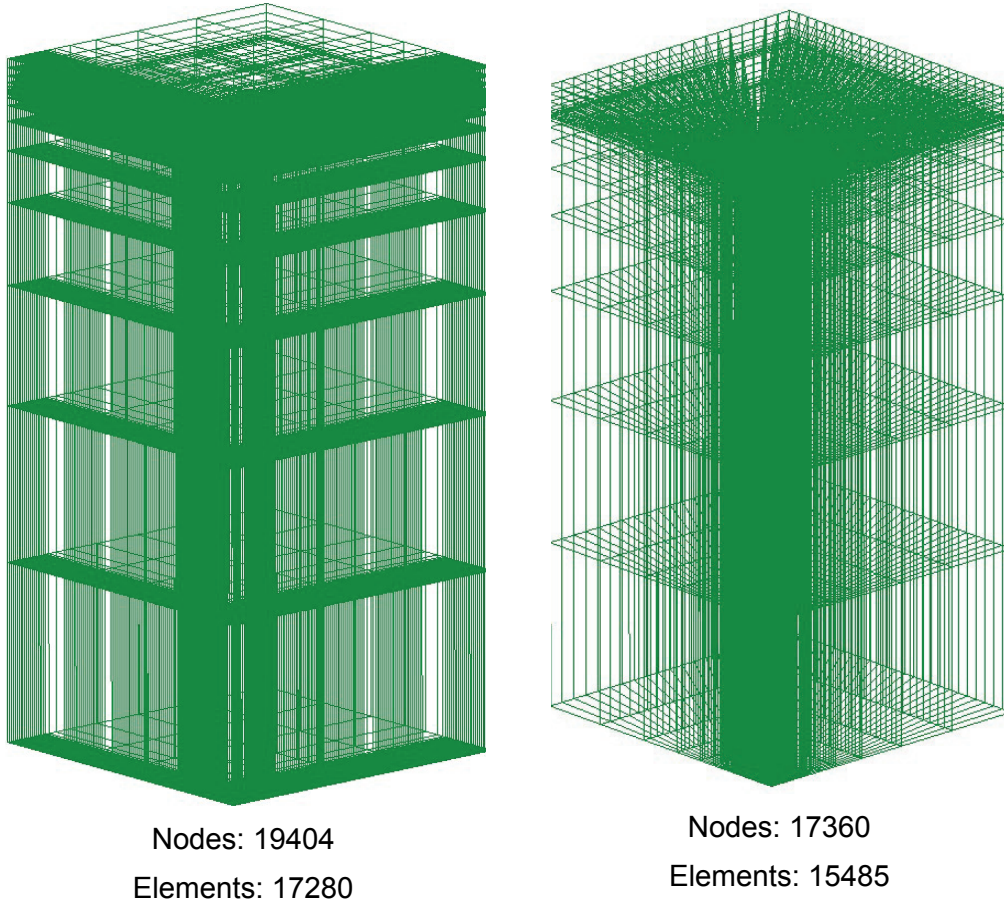


Figure 27: Meshes for the Far-Field Coupled T-M Model

4.2 RESULTS FROM FAR-FIELD MODEL

The results from the far-field numerical simulation of the repository with finite horizontal dimensions are presented in this section. The modelled results include temperatures, thermally induced stresses, total thermal and in-situ stresses, and thermally induced displacements at selected locations.

4.2.1 Thermal Results from Far-Field Model

Figure 28 illustrates the temperatures at three different locations O, P and Q shown in Figure 24. The peak temperature of 42.7°C occurs at 1,200 years at the repository. The maximum temperatures at the centre of a repository edge and repository corner are 27.6°C and 20.3°C, respectively, at 4,000 years after placement.

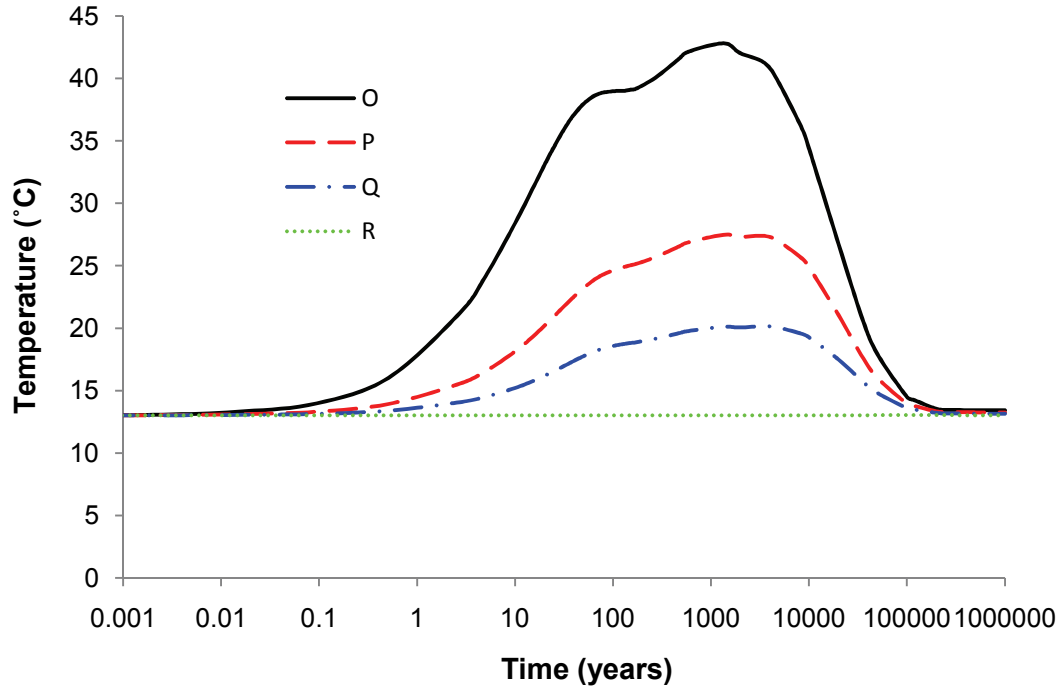


Figure 28: Temperatures at Three Different Locations of Points O, P and Q (for location see Figure 24)

Figure 29 shows the temperature versus distance from the repository centre along horizontal line OR at seven different times. The thermal load from the repository influences the temperature of the rock to a distance of about 2,000 m from the centre of the repository. Therefore, the horizontal dimensions of 5,000 m of the model are sufficient to conduct the far-field modelling.

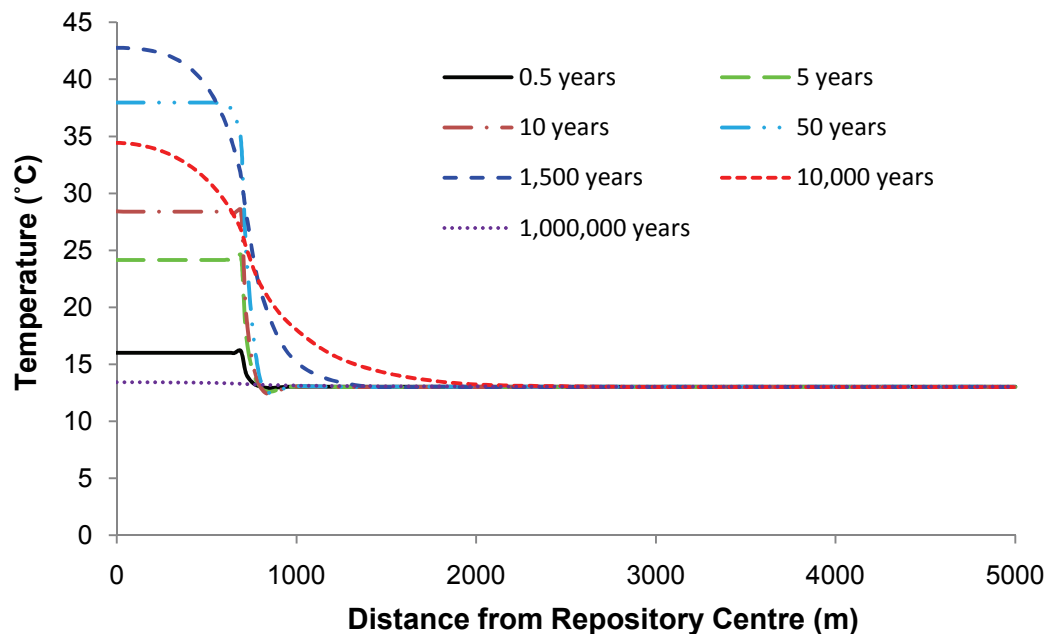


Figure 29: Temperatures versus Distances from Repository Centre along Horizontal Line OR through the Repository Model (for location see Figure 24)

Temperature profiles and the temperature rise along the vertical axis through the centre of the repository as shown in Figure 24 at different times are shown in Figures 30 and 31, respectively. The thermal influence of the DGR only appears to reach a maximum depth of 2,500 m at 10,000 years after repository closure.

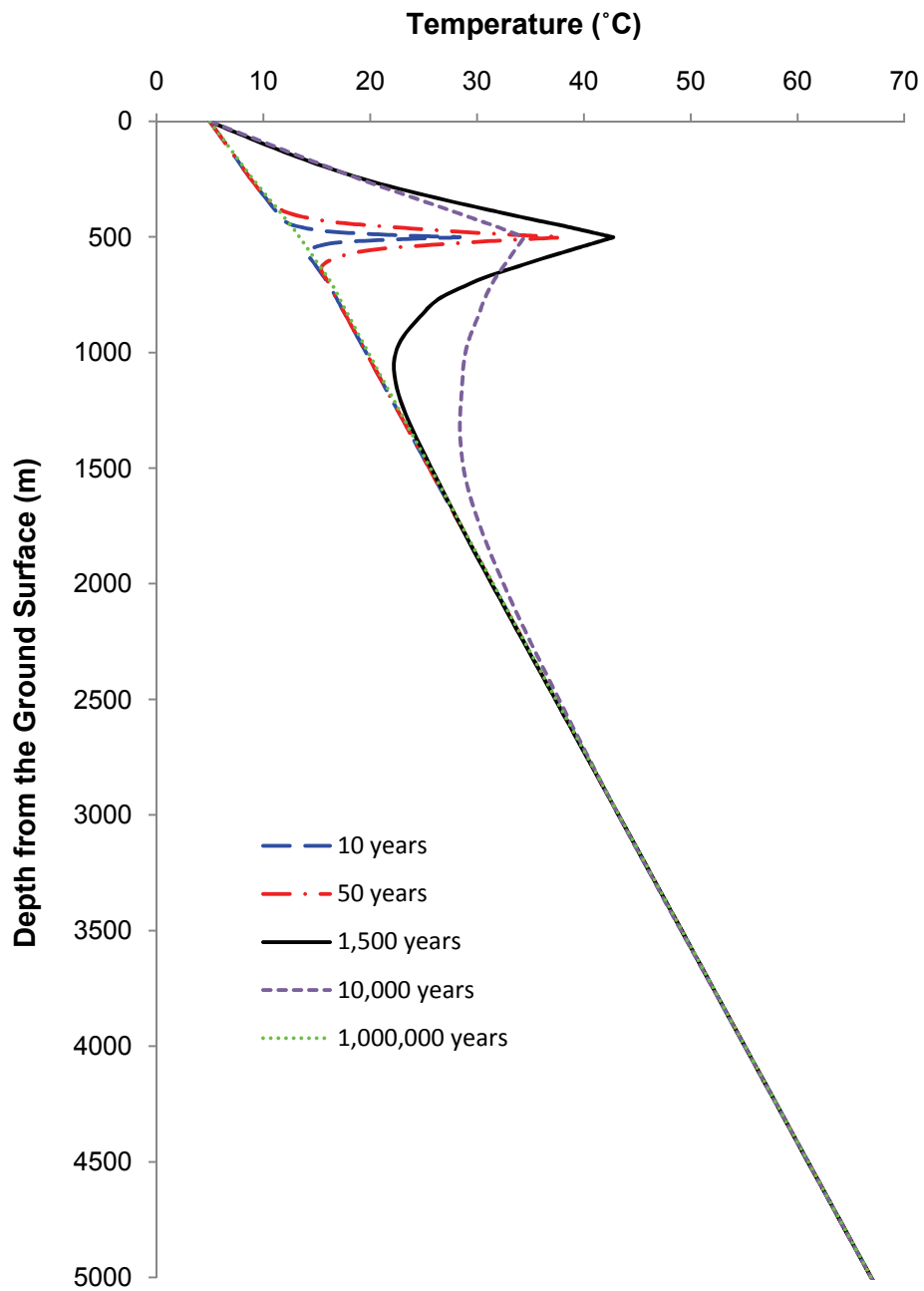


Figure 30: Temperatures along Vertical Line AE (for location see Figure 24) at 5 Times following Repository Closure

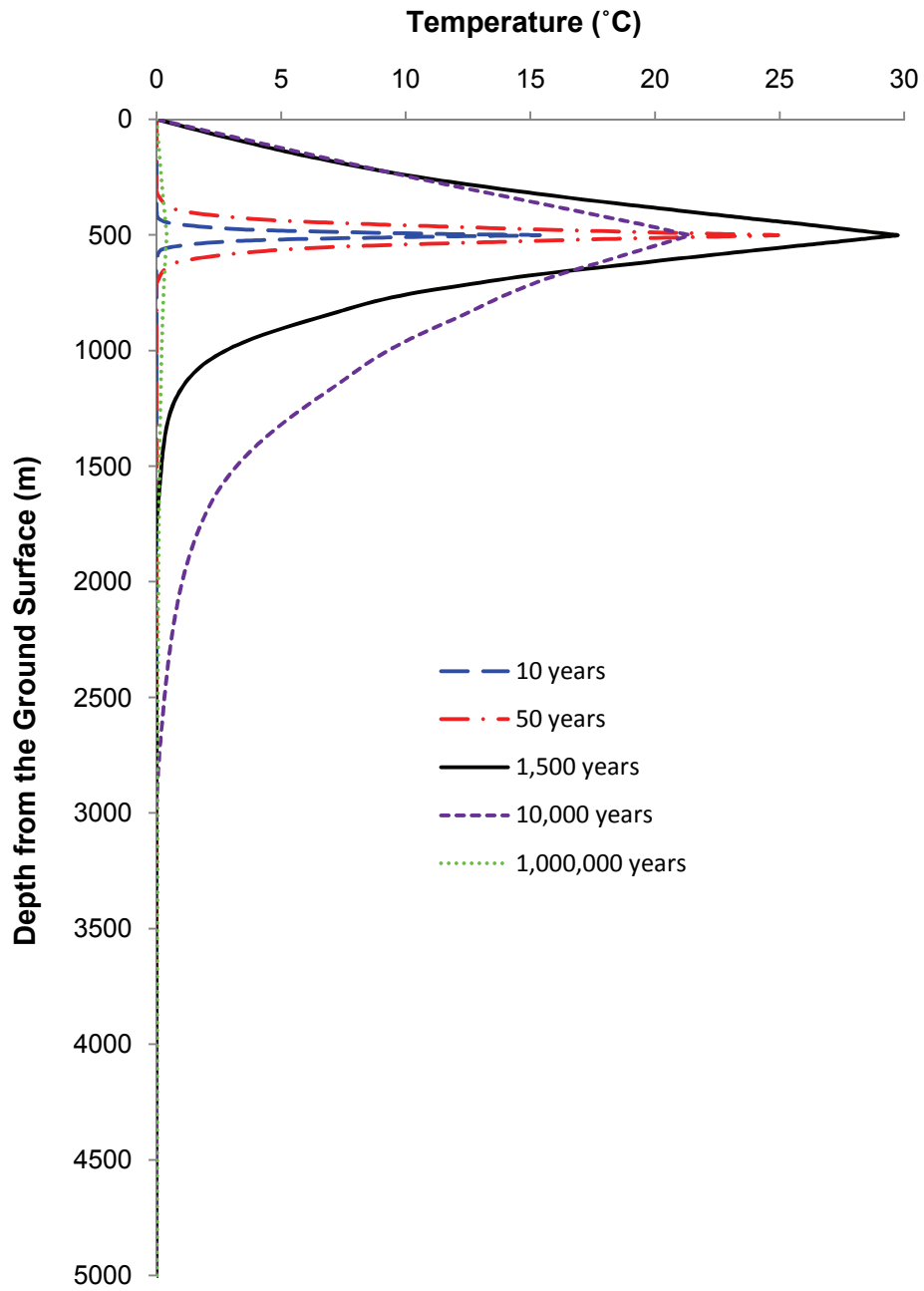


Figure 31: Thermally Induced Temperature Rise along Vertical Line AE (for location see Figure 24) at 5 Times following Repository Closure

Temperatures versus time at selected points along the vertical line through the repository centre are shown in Figure 32. At a location of 2,700 m below the ground surface, the temperature rise is only 0.6°C at 35,000 years after placement.

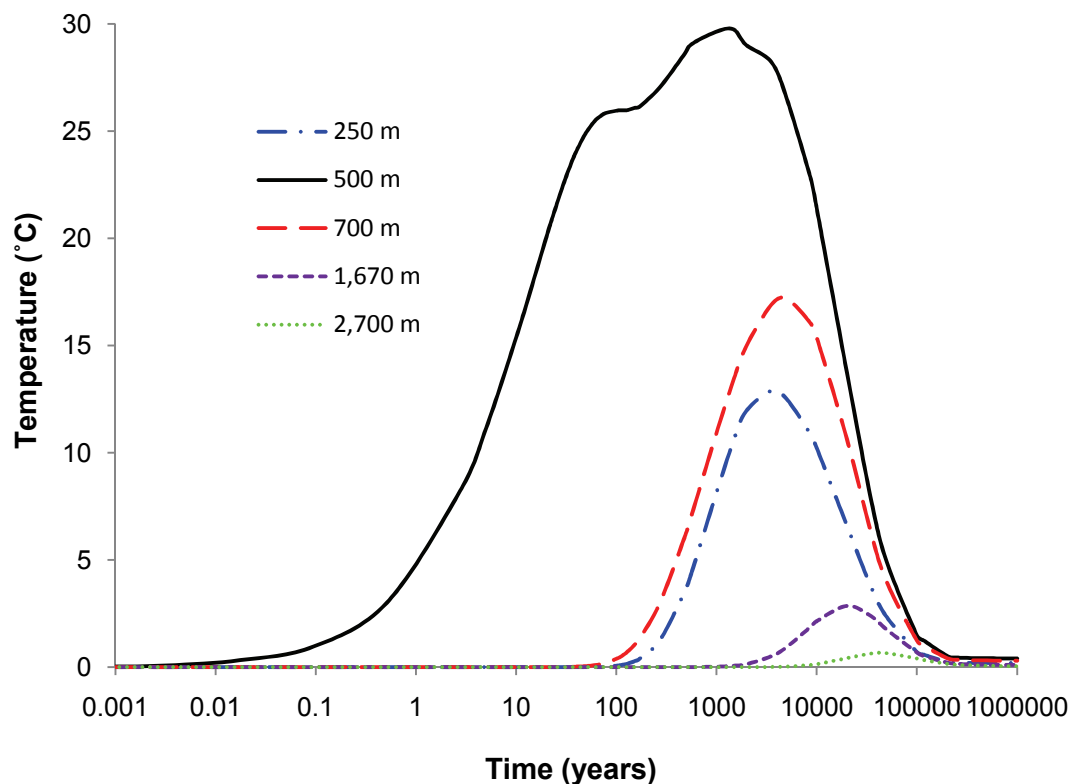


Figure 32: Temperature Rise induced only by Used Nuclear Fuel in a Repository at Different Depths below Ground Surface along Vertical Line AE (for location see Figure 25)

Figure 33 shows the temperature contours in the rock around the repository at six different times. At 100,000 years, temperatures in the rock will have returned to its initial temperatures. As there is no significant thermal influence below approximately 2700 m depth, Figure 33 was truncated at 2812 m depth to provide for production of a more visually informative plot.

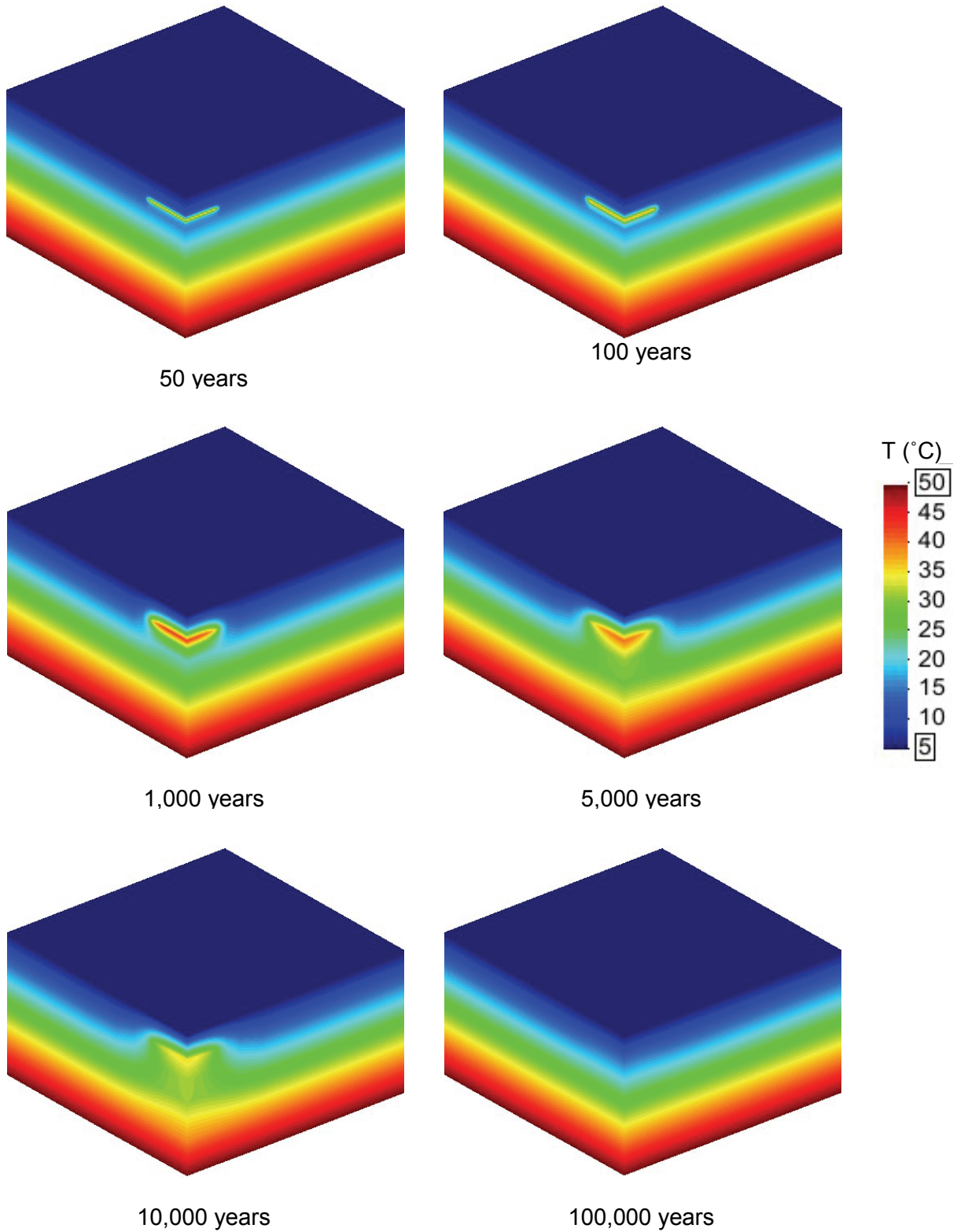


Figure 33: Temperature Response at 6 Different Times (The base of these figures is located at 2812 m below ground surface)

4.2.2 Mechanical Results from Far-Field Model

4.2.2.1 Thermally Induced Vertical Displacements

Figure 34 shows the thermally induced vertical displacements versus time at four different locations along the vertical axis through the repository centre. On the ground surface, the peak vertical displacement at 5,000 years after placement is 134 mm, which is very small in comparison with crustal depression due to glacial ice load, which is anticipated to be in the order of 10s of meters (Brevik and Reid 2000). At 500 m from the ground surface (repository centre), the peak vertical displacement is 125 mm at 10,000 years after placement. At 4,500 m from the ground surface, the peak vertical displacement is 3 mm after 10,000 years of waste placement.

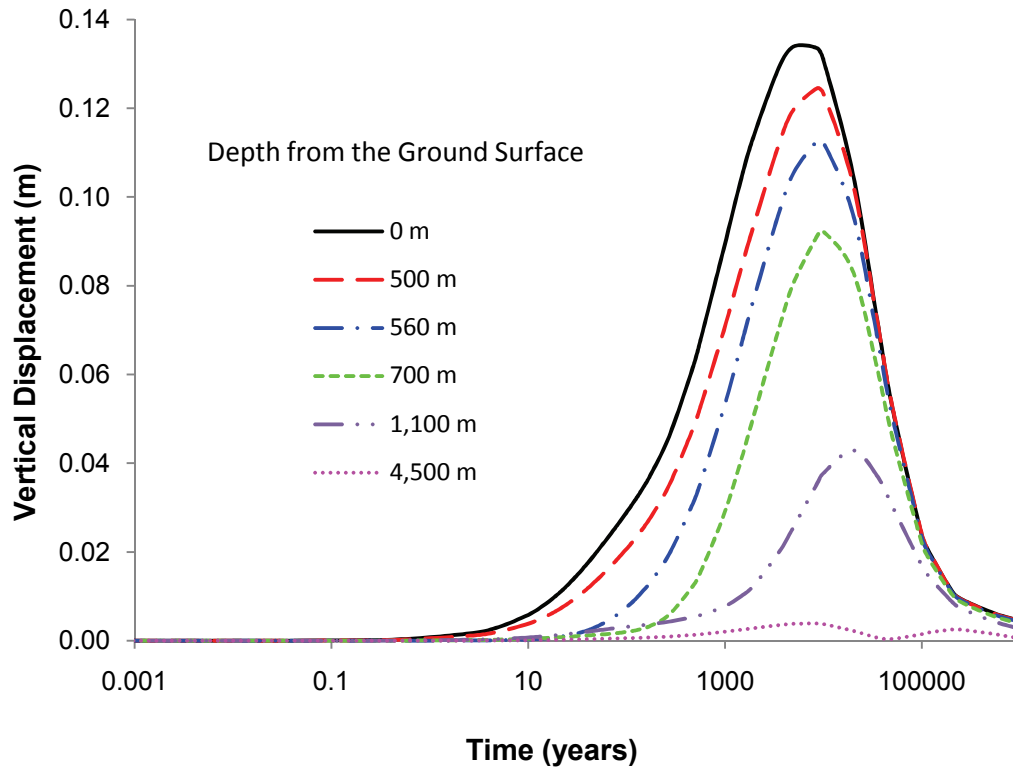


Figure 34: Vertical Displacements versus Time at Different Locations along Vertical Line AE running through the Repository (for location see Figure 24)

Figure 35 shows the vertical bedrock displacements versus the depth from the ground surface at six different times. Deeper than 1,700 m, the vertical displacements are less than 0.02 m.

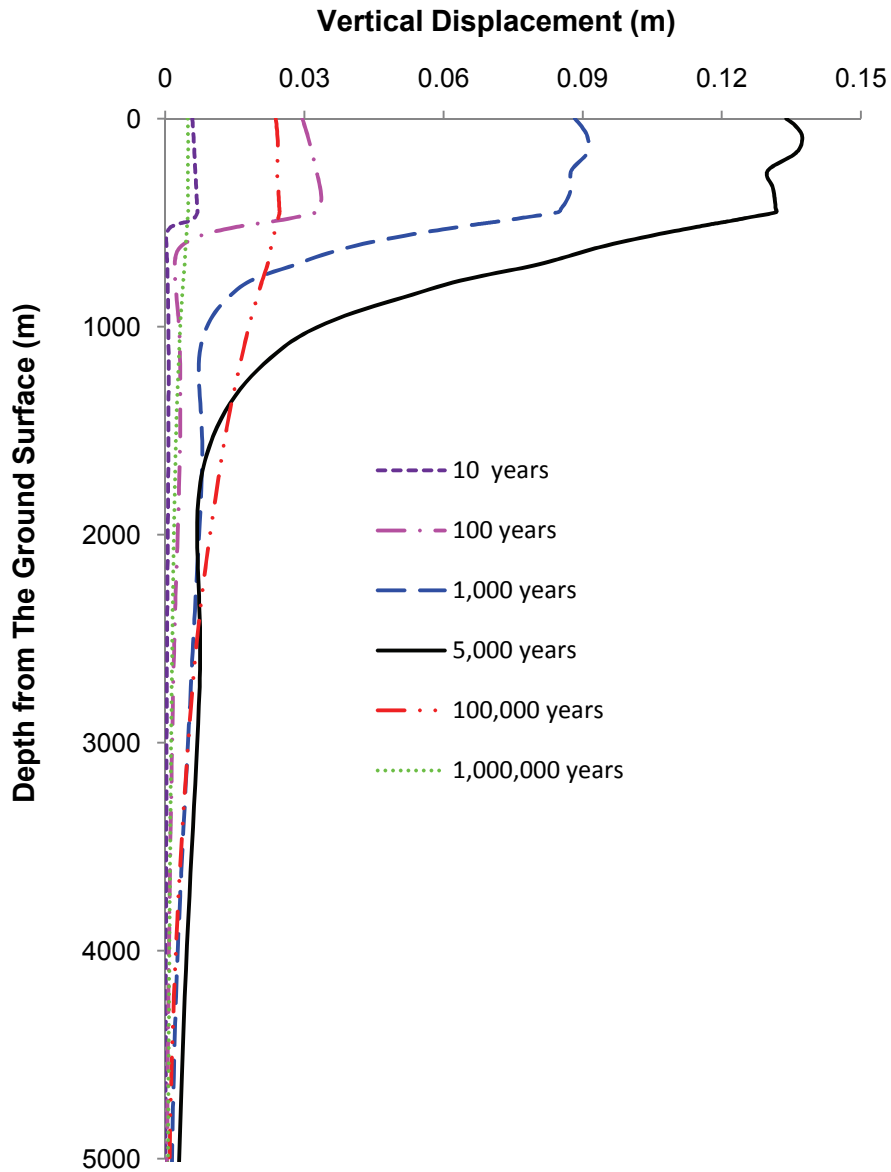


Figure 35: Vertical Displacements along Vertical Line AE (for location see Figure 24) at Different Times

The vertical displacements versus time at three different locations A, P' and B (see Figure 24 for locations) are shown in Figure 36. At the location P', which is on the ground surface above the mid-edge of the repository, the vertical displacement is about 95 mm at 5,000 years after placement. At Point B, the vertical displacement is only 8 mm at 100,000 years of placement. Figure 37 shows the vertical displacement versus distance from the repository centre along the horizontal line of AB. The obvious influence of thermally induced displacements only occurs at the range of 4,000 m horizontally from the repository centre during the first 10,000 years after repository closure.

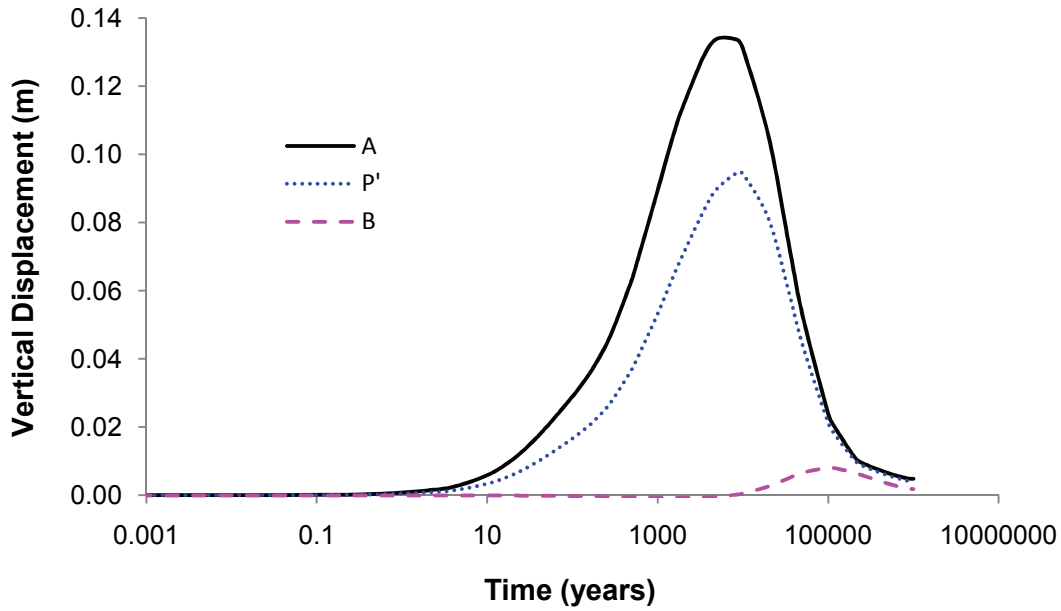


Figure 36: Vertical Displacements at Points A, P', and B of Repository Site (see Figure 24 for locations)

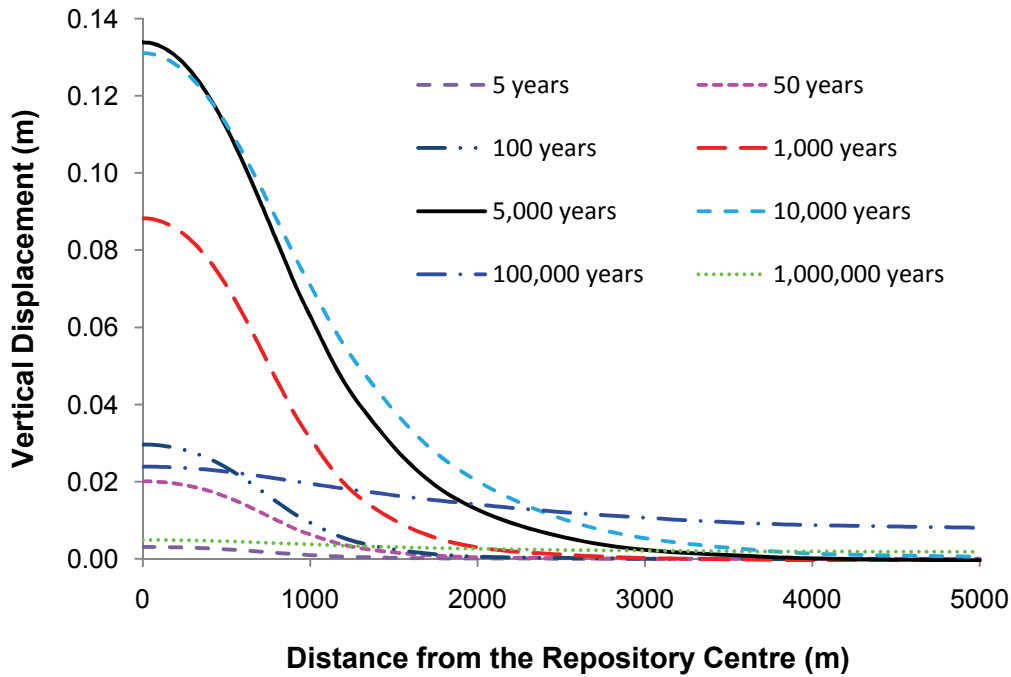


Figure 37: Vertical Displacements along Line AB at Different Times (see Figure 24 for location of this line at the repository site)

The vertical displacements in a three-dimensional model at a time of 5,000 years after waste placement are shown in Figure 38. The rock below and above the repository is lifted due to thermal expansion.

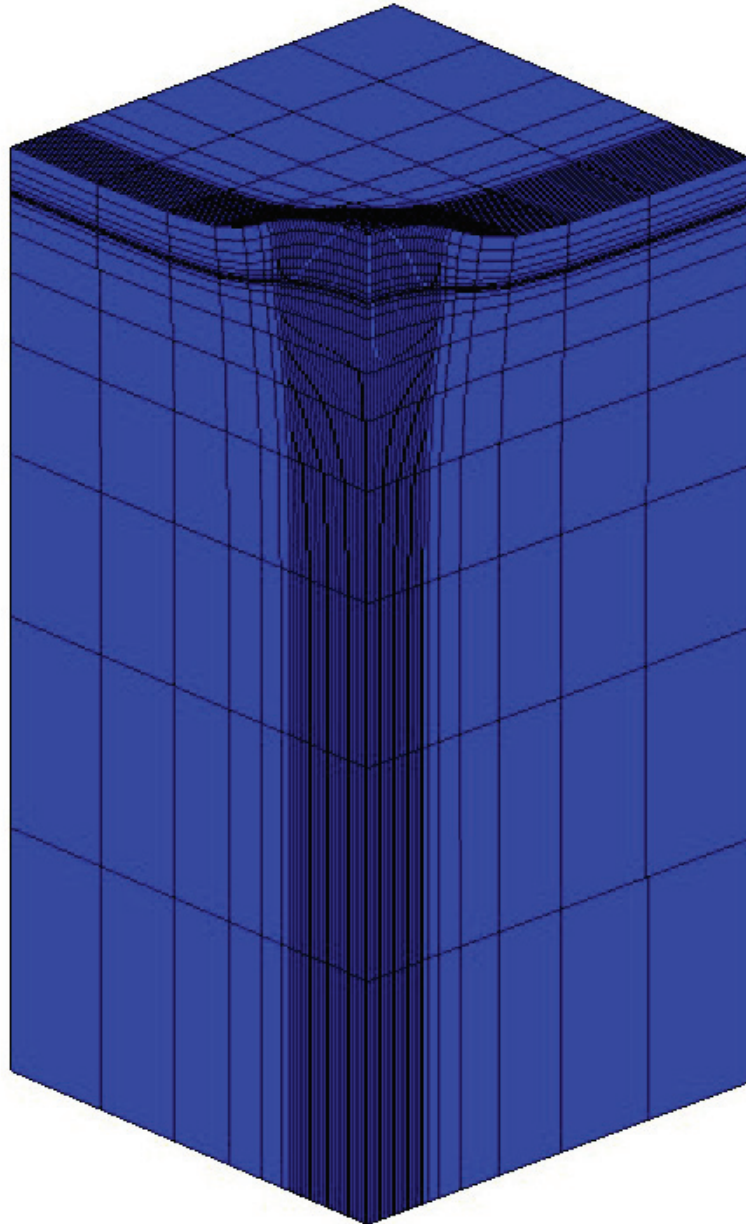


Figure 38: Thermally Induced Vertical Displacements at 5000 Years with a Maximum Value of 0.14 m (Note: The vertical displacement scale is exaggerated (factor = 5,000) for clarity)

4.2.2.2 Thermally Induced Stresses

Due to the symmetry of the model, the stresses in the X-, Y-, and Z-directions are the major stresses. The thermally induced stresses in the X-, Y-, and Z-directions along Line OR (horizontal line from repository centre to model boundary shown in Figure 24) are shown in Figures 39, 40 and 41. The peak thermally induced stresses in the X-, Y- and Z- directions are about 7.0 MPa, 7.5 MPa and 0.8 MPa at 500 years, 500 years and 5,000 years, respectively. The thermally induced stress changes mostly occur at the area of repository.

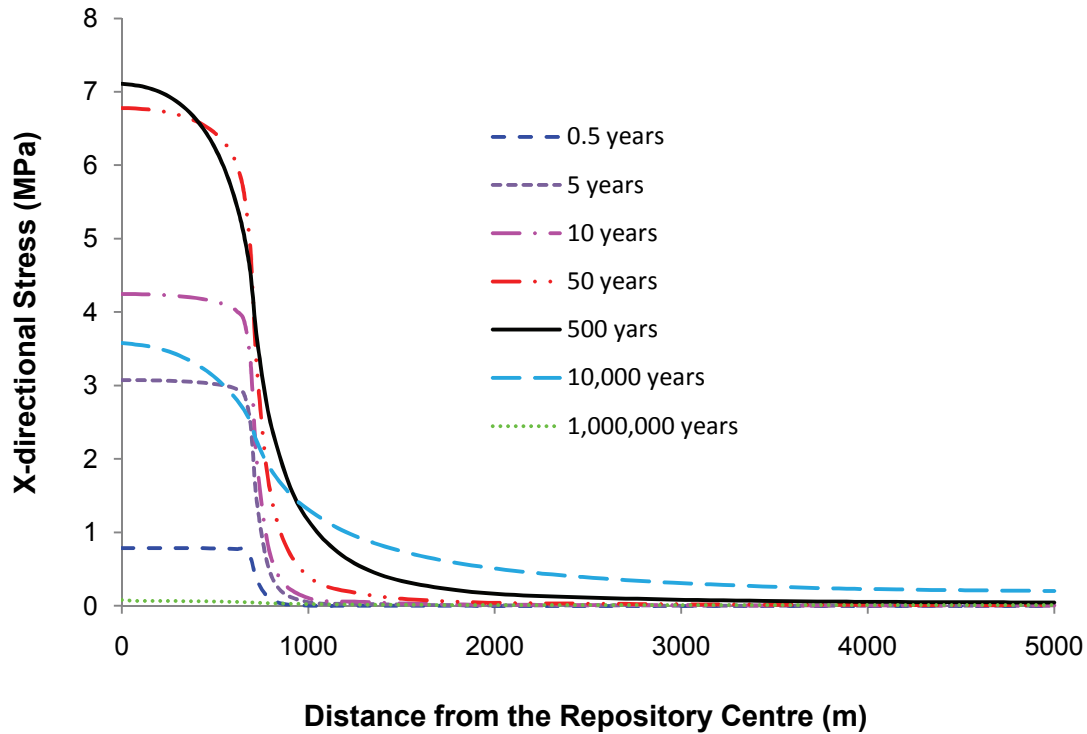


Figure 39: Thermally Induced Stresses in X-direction along Horizontal Line OR at Repository Level (for location see Figure 24)

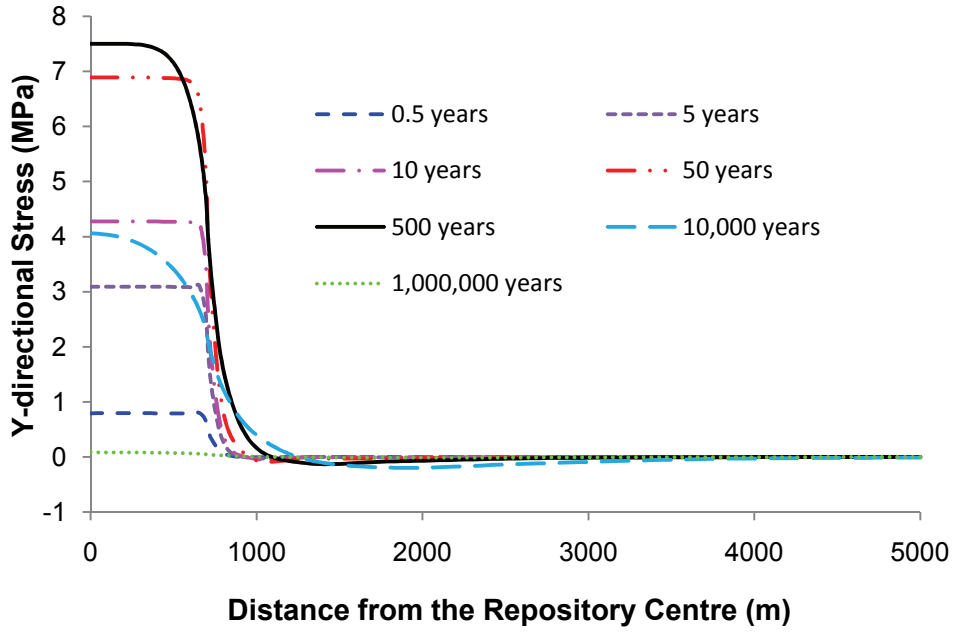


Figure 40: Thermally Induced Stresses in Y-direction along Horizontal Line OR at Repository Level (for location see Figure 24)

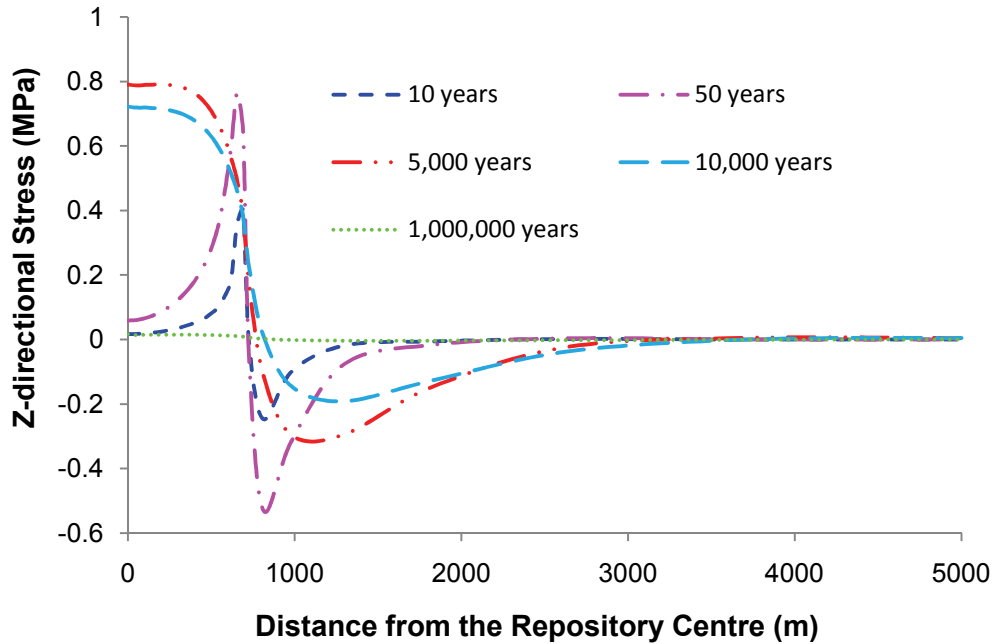


Figure 41: Thermally Induced Stresses in Z-direction along Horizontal Line OR at Repository Level (for location see Figure 24)

Profiles of the thermally induced stresses in the X-, Y-, and Z-directions along line AE (the vertical centreline of the repository as shown in Figure 24) are shown in Figures 42, 43 and 44. The greatest thermally induced compressive stresses in the X- and Y-directions are about 6.8 MPa and 7.3 MPa at 1,000 years after waste placement, respectively. The greatest thermally induced tensile stress in the X- and Y-directions along the vertical line is 3.5 MPa and 2.8 MPa at the ground surface at 5,000 years, respectively.

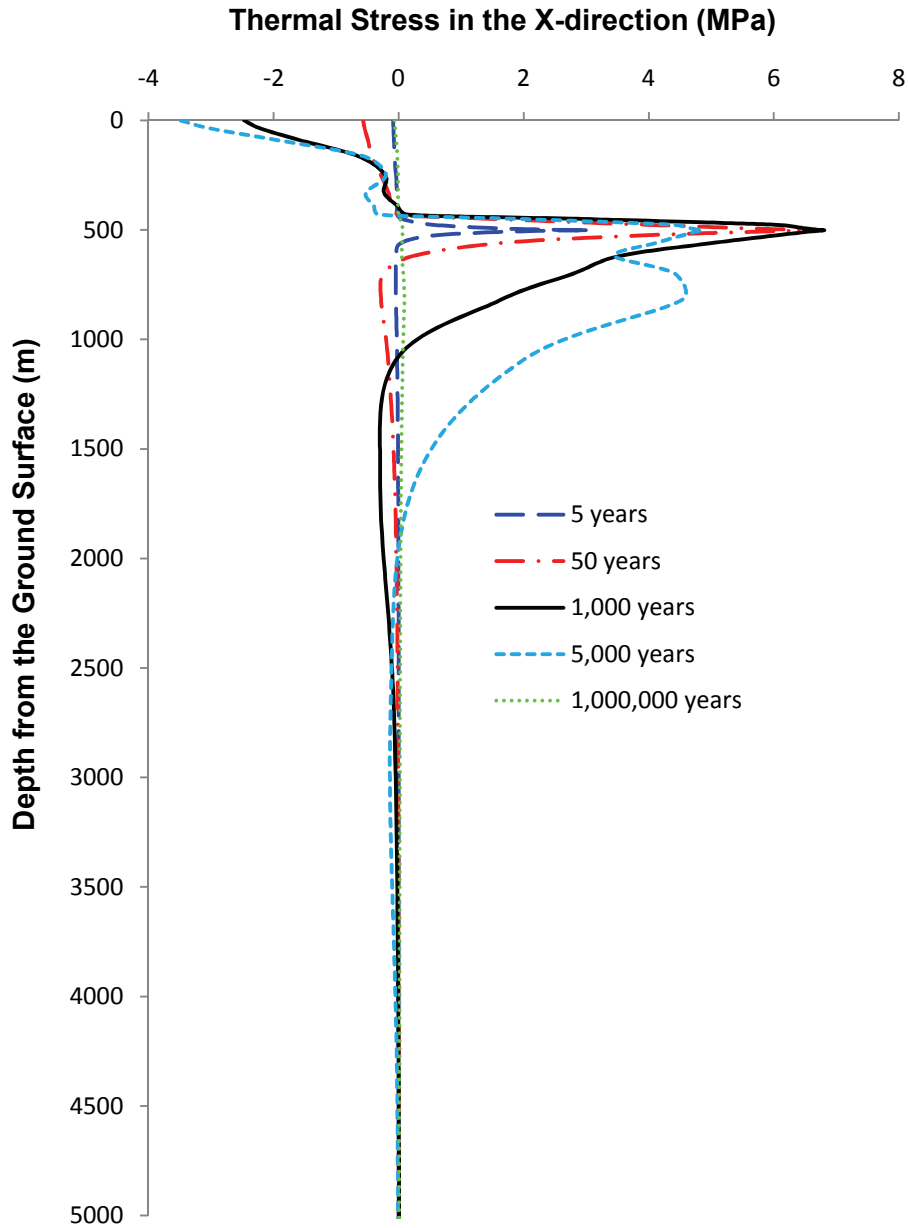


Figure 42: Thermally Induced Stresses in X-direction along Vertical Line AE through Repository (for location see Figure 24)

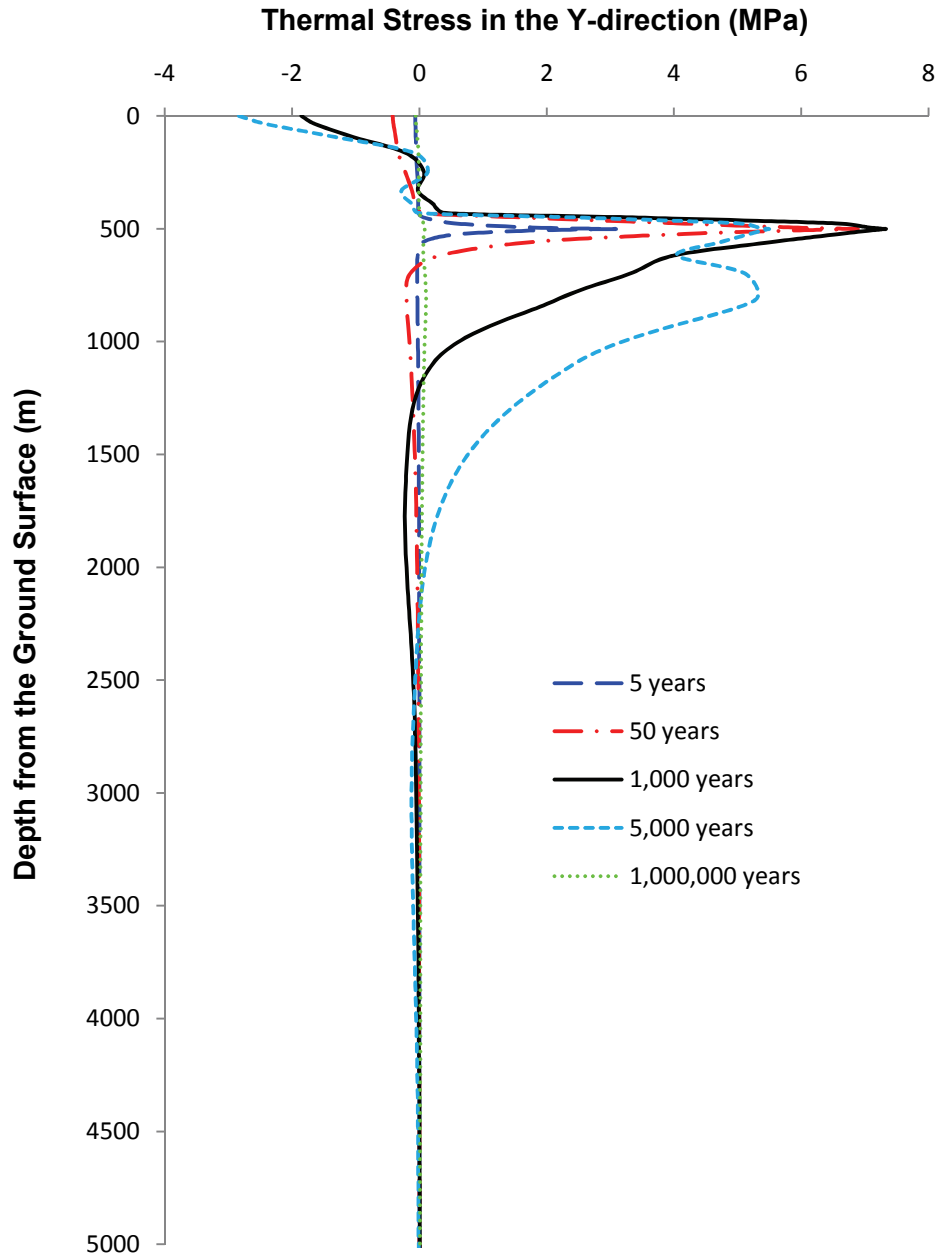


Figure 43: Thermally Induced Stresses in Y-direction along Vertical Line AE through Repository Centreline (see Figure 24 for location)

The thermally induced compressive stress in the Z-direction is about 1.1 MPa at 5,000 years. The thermally induced tensile stress in the Z-direction along the vertical line AE is about 0.15 MPa at about 2,700 m from the ground surface at 1,000 years.

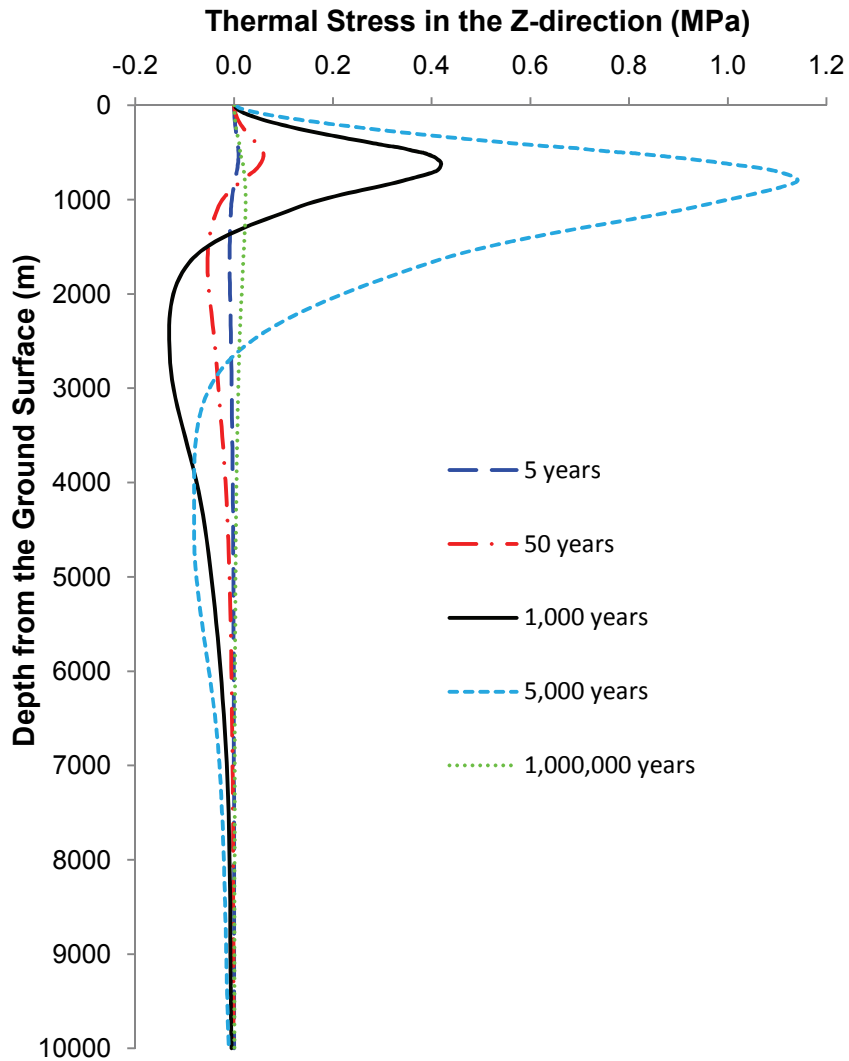


Figure 44: Thermally Induced Stresses in Z-direction along Vertical Line AE through Repository Line (see Figure 24 for location)

4.2.2.3 Total Stresses

The stability of rock mass is influenced by the total stresses and not the thermally induced stresses. Due to the symmetry of the model, the modelled stress components in the X-, Y-, and Z-directions are also the major stress components. Therefore, adding the thermally induced X-, Y-, and Z-directional stresses to the initial major stress components σ_2 (X-direction), σ_1 (Y-direction) and σ_3 (vertical direction) (as shown in Table 1) can obtain the major stress components in the X-, Y-, and Z-directions, respectively. The excavation-induced stresses are irrelevant for the far-field analyses because the far-field modelling is focused on the uplift of the rock mass induced by thermal expansion. The excavation-induced stresses are analyzed in the near-field modelling in Section 3.2. Figures 45, 46 and 47 show the total stresses in the X-, Y- and Z-directions along the horizontal line OR at different times. There is no tensile stresses in

the rock in the X-, Y- and Z-directions at any time along the horizontal line OR. The maximum and minimum major stresses at the repository are the Y-directional stress and vertical stress, respectively. Using Eq (1), the stress strength (the major principal stress at failure) can be calculated. It is more than 80 MPa. Therefore, there is no thermally induced damage at any time.

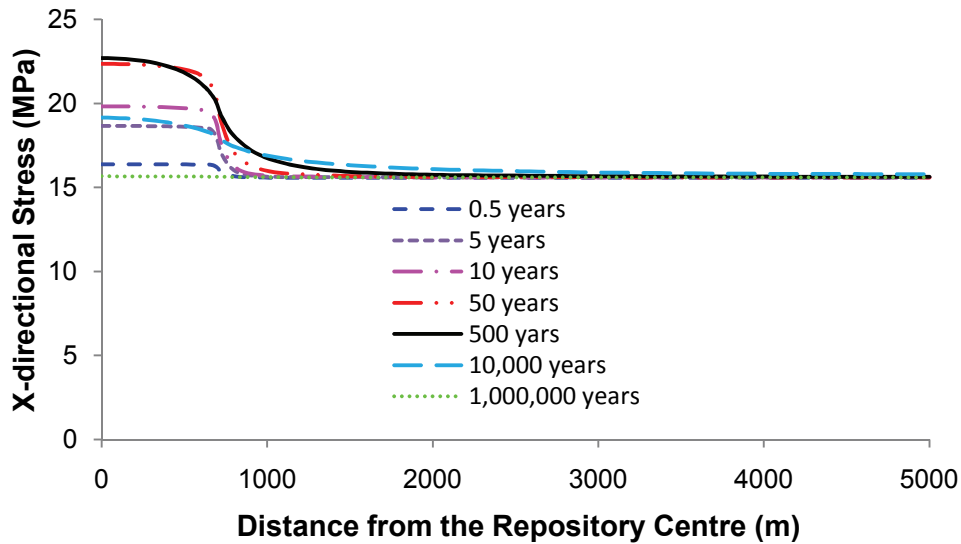


Figure 45: Total Stresses in X-direction along Horizontal Line OR (see Figure 24 for location) at Different Times

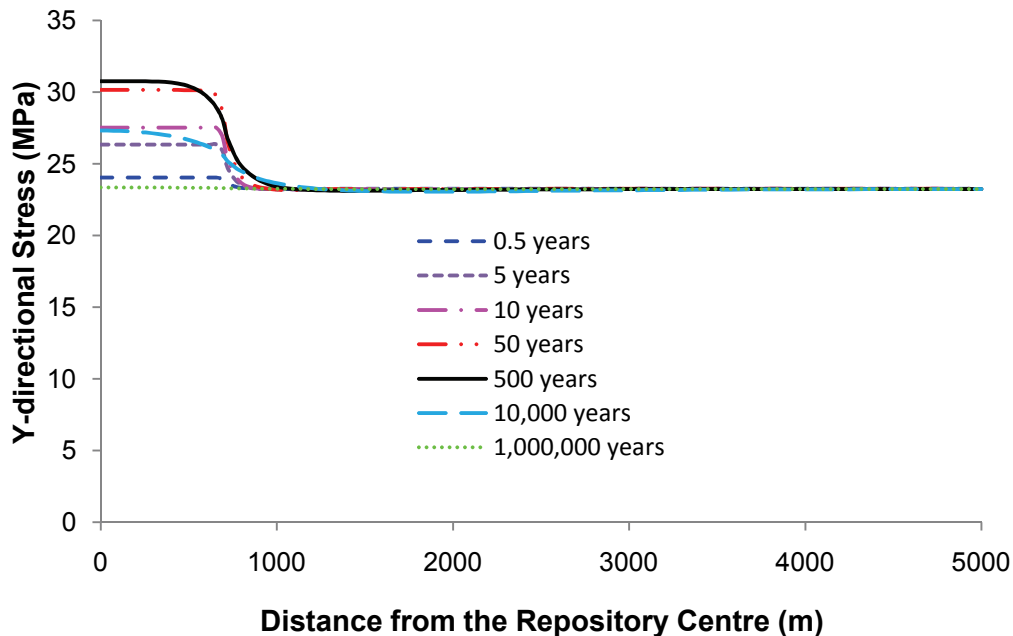


Figure 46: Total Stresses in Y-direction along Horizontal Line OR (see Figure 24 for location) at Different Times

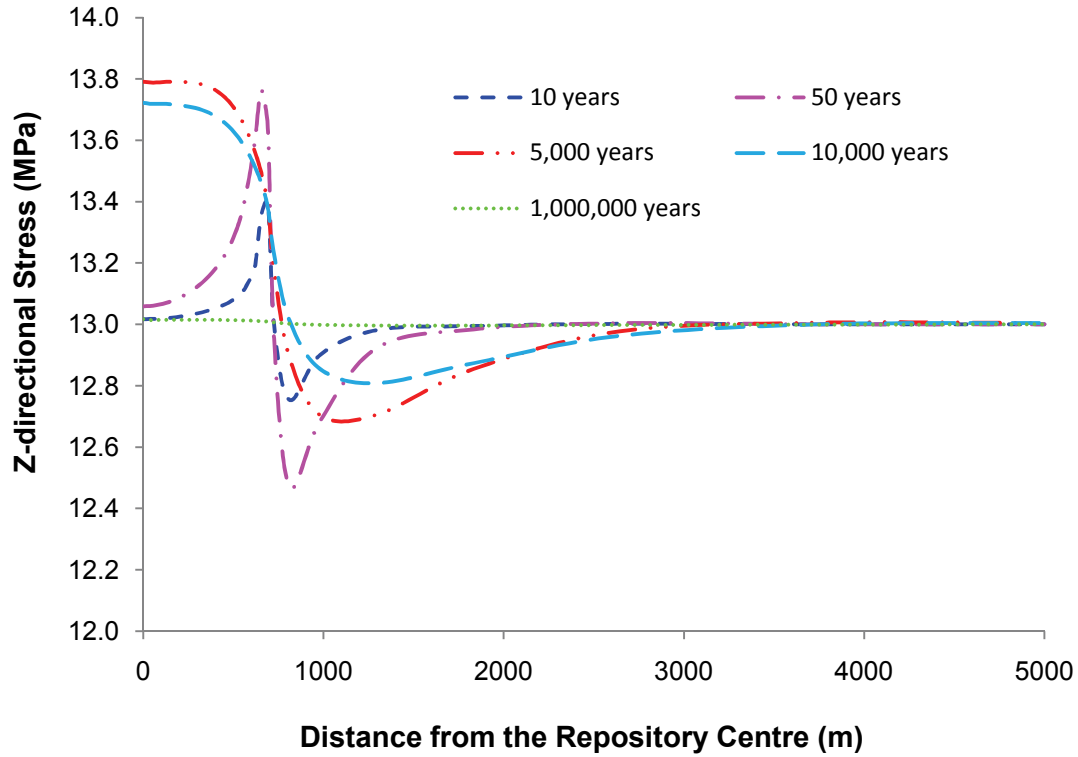


Figure 47: Total Stresses in Z-direction along Horizontal Line OR (see Figure 24 for location) at Different Times

The total stresses in the X-, Y- and Z-directions along vertical line AE are shown in Figures 48, 49 and 50. There is no tensile stress in the X-, Y- and Z-directions at any depth and at any times along vertical line AE through the repository centre (see Figure 24).

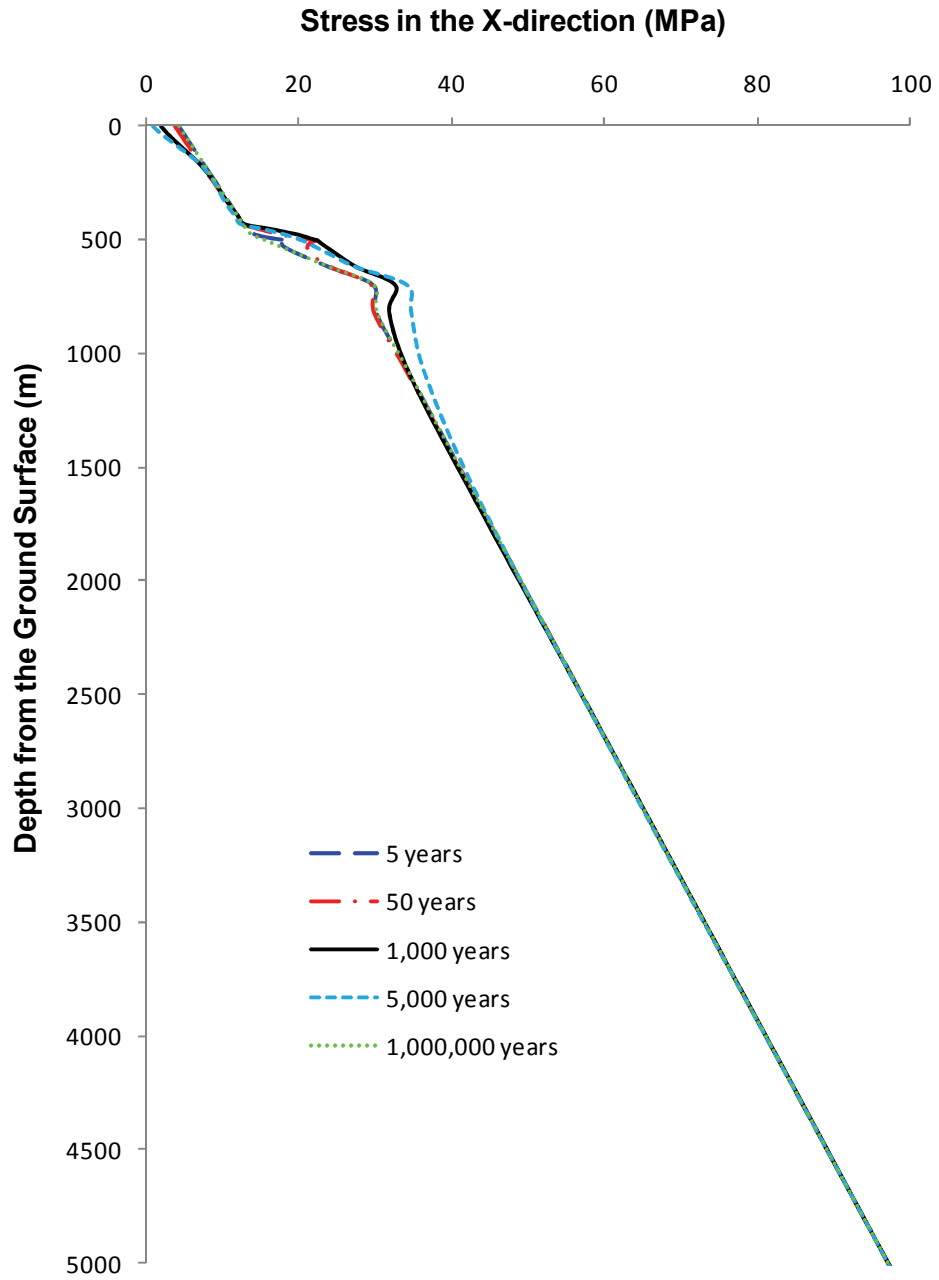


Figure 48: Total Stresses in X-direction along Vertical Line (AE in Figure 24) at Different Times

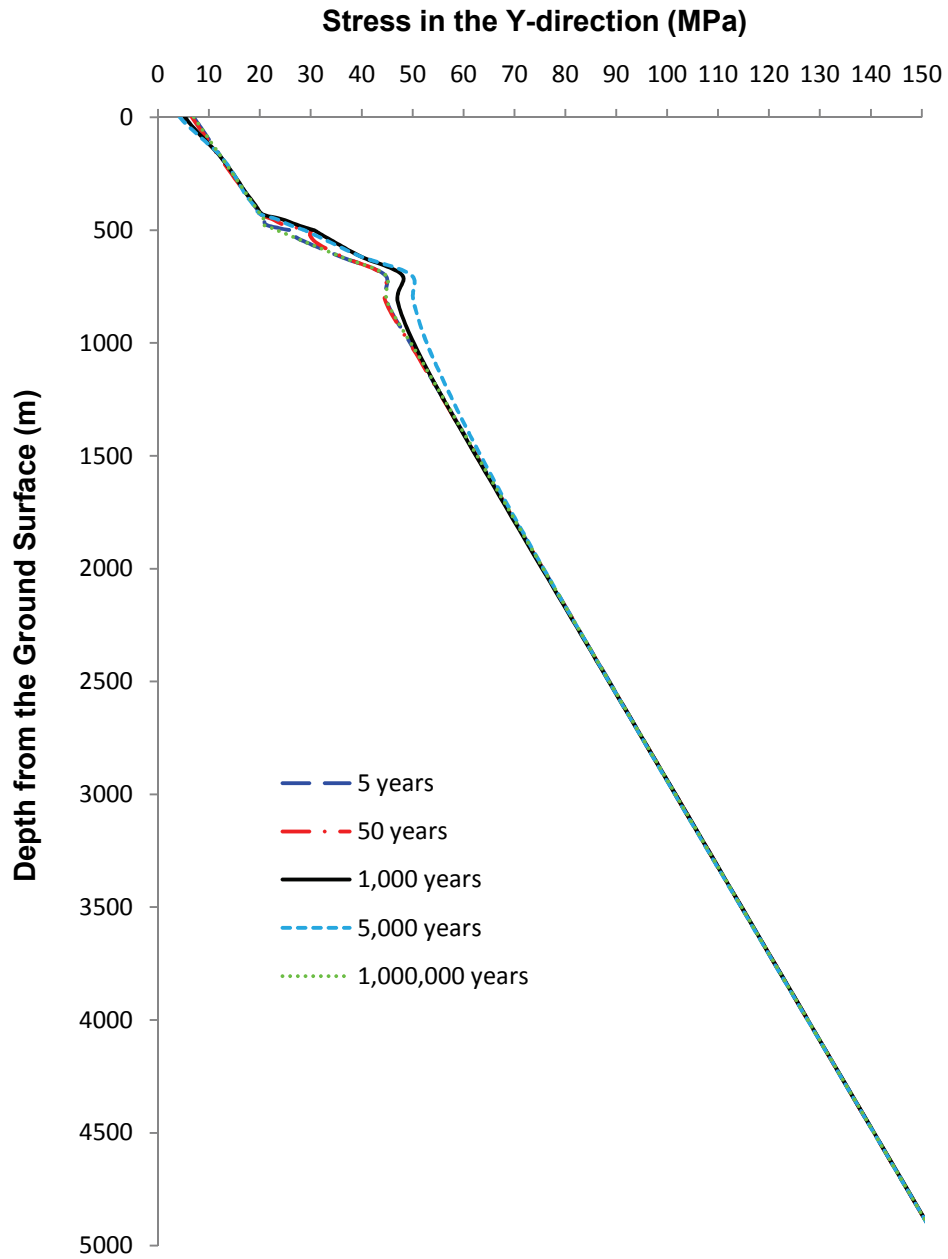


Figure 49: Total Stresses in Y-direction along Vertical Line (AE in Figure 24) at Different Times

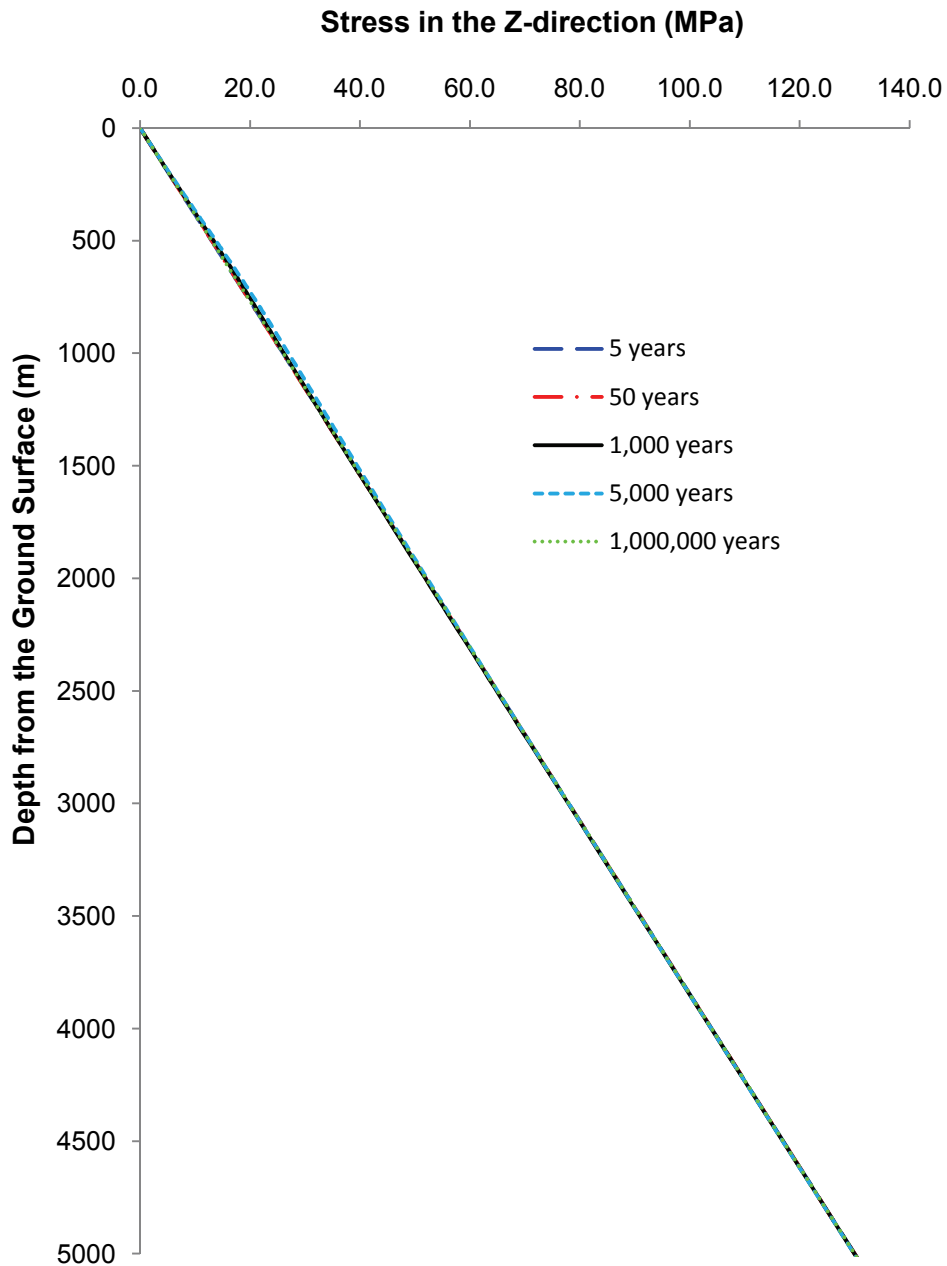


Figure 50: Total Stresses in Z-direction along Vertical Line (AE in Figure 24) at Different Times

At depth less than 1,000 m, the maximum and minimum major stresses are the Y-directional stress and the vertical stress, respectively. Using Eq (1) and based on the parameters of Hoek and Brown failure criterion for shale, limestone and granite described in Section 2.3, the rock mass strength versus depth can be calculated as shown in Figure 51. If one compares maximum stress with stress strength, there would be no thermally induced damage along the vertical line if the rock mass were assumed to be homogeneous and intact.

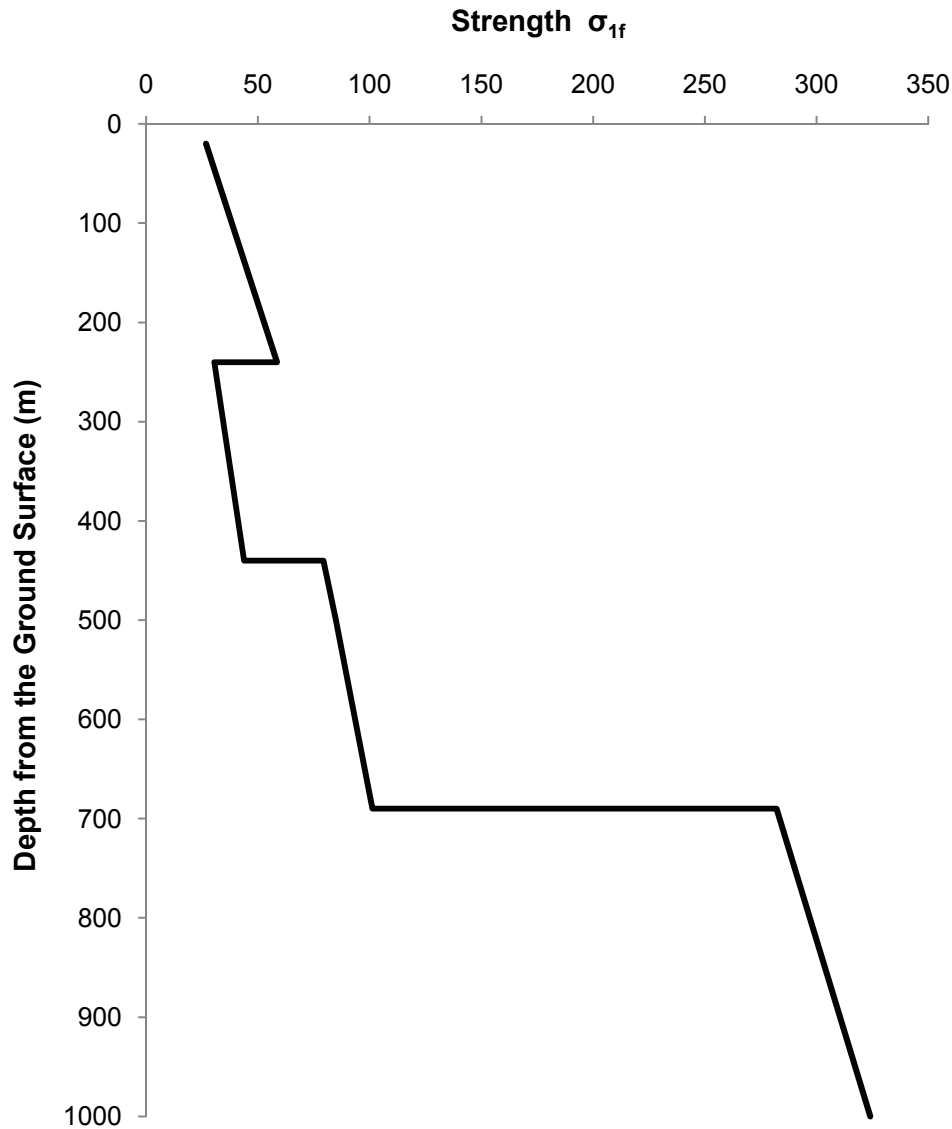


Figure 51: Rock Mass Strength versus Depth from the Ground Surface

4.2.3 Summary of Far-field T-M Modelling of Repository

A series of numerical simulations of a repository that uses the HTP method in a sedimentary host rock has been completed using CODE_BRIGHT. Material properties relevant to the components of the UFC, buffer and host rock were used to determine if any seriously adverse T-M related effects could be identified for this concept.

The thermal response in the rock surrounding a closed DGR constructed using HTP geometry was determined to be as follows.

- The peak temperature in the rock is 42.7°C at the centre of the repository after 1,200 years.

- The peak temperatures at the centre of the repository edge (727.5 m from repository centreline) and repository corner (1,265 m from repository centreline) are 27.6°C and 20.3°C, respectively, at 4,000 years after placement.
- There is no influence on the temperature of the rock at the model's edge (5,000 m from the repository centre).
- The repository does not influence the temperature of the rock beyond 2,500 m from the ground surface.
- The repository induced temperature increase in the rock will not be more than 30°C at any location.
- After 1,000,000 years there is no discernible thermal influence of the repository.

The thermally induced mechanical responses of a repository located in an intact rock mass are as follows.

- The greatest thermally induced vertical displacement on the top above the repository is about 0.134 m at 5,000 years after waste placement.
- At 500 m depth (repository centre), the peak vertical displacement of the repository is about 125 mm at 10,000 years after waste placement.
- The greatest thermally induced stresses in the X-, Y- and Z-directions are 7 MPa, 7.5 MPa and 0.8 MPa at the repository centre.
- The greatest thermally induced tensile stresses in the X- and Y-directions are 3.5 MPa and 2.8 MPa, respectively, and occur at the ground surface.
- There is no tensile total stress in the rock mass near the repository in any directions and at any time.

5. SUMMARY OF THE RESULTS

A series of thermal-only or coupled T-M modelling was successfully performed using CODE_BRIGHT to gain an initial understanding of what the behaviour of the rock mass might be in the near-field and far-field of a DGR for used nuclear fuel using the HTP method. From the near-field, the following conclusions are obtained from the CODE_BRIGHT simulations.

- The highest temperature on the container surface is 117°C, which is less than the requirement for the HTP repository concept (120°C).
- The thickness of the buffer that does not experience temperatures above 100°C is 0.477 m.
- The highest temperature at the tunnel surface is 69°C.
- Tunnel excavation will potentially induce a damage zone with a thickness of 0.053 m near the tunnel roof.
- The thicknesses of the damaged rock are 0.211 m and 0.077 m at the tunnel roof and the tunnel wall, respectively, 1,000 years after used nuclear used fuel placement without considering the swelling pressure of buffer.

From the far-field modelling component of this work, the following conclusions are obtained.

- The greatest thermally induced uplift at the ground surface is less than 0.134 m.
- Thermally induced stresses in the rock mass near the repository are less than 7.5 MPa in all directions.
- There are no tensile total stresses in the rock mass near the repository.

- Based on the rock strength of the rock near the repository, there will not be any additional fractures induced by the thermal response caused by used nuclear fuel.
- Because there is no variable stress boundary application in the present version of CODE_BRIGHT, the initial in-situ stress cannot be applied in the far-field model. Therefore, the total stresses have to be obtained manually by combining the thermally induced stresses and the in-situ stresses.
- For the present version of CODE_BRIGHT, thermal load cannot be applied using thermal density. It can only be applied at nodes. Therefore, it is a big effort to apply the thermal load to many different nodes for many time steps

The results of the modelling using CODE_BRIGHT indicate that there is a layer of damage zone at the tunnel roof immediately after tunnel excavation. Therefore, it may be necessary to supply a light supporting system to ensure excavation stability. Far-field modelling indicates that there are no adverse effects from the existence of a DGR in the limestone at 500 m depth using the HTP method on the geosphere in the mechanical point of view.

Future work that should be done to improve confidence in these results includes (1) improving CODE_BRIGHT to include the variable boundary conditions and application of thermal load using heat density on a certain volume; and (2) running the far-field coupled T-M model with application of non-zero initial stresses using improved CODE_BRIGHT as required in (1).

ACKNOWLEDGEMENTS

The author would like to acknowledge the AECL reviewers for their input.

REFERENCES

- Baumgartner, P. 2005. Scoping analyses for the design of a deep geologic repository in sedimentary rock. Ontario Power Generation, Nuclear Waste Management Division Report, 06819-REP-01300-10093-R00.
- Brevik, E.C and Reid, J.R. 2000. Uplifted-based limits to the thickness of ice in the Lake Agassiz basin of North Dakota during the Late Wisconsinan. *Geomorphology* 32: 161-169.
- CODE_BRIGTH User's Guide. 2009. Geotechnical Engineering Department, Technical University of Catalunya, Spain (digital format available at http://www.etcg.upc.edu/research/code_bright).
- COMSOL Multiphysics user's guide - COMSOL 3.5a. 2008. COMSOL AB.
- Graham, J., Saadat, F., Gray, M.N., Dixon, D.A. and Zhang, Q.-Y. 1989. Strength and volume change behaviour of a sand-bentonite mixture. *Canadian Geotechnical Journal* 26, 292-305.
- Guo, R. 2007. Numerical modelling of a deep geological repository using the in-floor borehole placement method. Nuclear Waste Management Organization NWMO TR-2007-14. (available at www.nwmo.ca).
- Guo, R. 2008. Sensitivity analyses to investigate the influence of the container spacing and the tunnel spacing on the thermal response in a deep geological repository. Nuclear Waste Management Organization NWMO TR-2008-24. (available at www.nwmo.ca).
- Guo, R. 2009. Application of numerical modelling in choosing container spacing, placement-room spacing and placement-room shape for a deep geological repository using the in-floor borehole placement method. Nuclear Waste Management Organization NWMO TR-2009-28. (available at www.nwmo.ca).
- Maak, P. and G.R. Simmons. 2001. Summary report: a screening study of used-fuel container geometric designs and emplacement methods for a deep geologic repository. Ontario Power Generation, Nuclear Waste Management Division Report 06819-REP-01200-10065-R00.
- NAGRA. 1985. Projekt Gewähr, nuclear waste management in Switzerland – Feasibility studies and safety analysis. Nationale Genossenschaft für die Lagerung Radioaktiver Abfälle Report, NAGRA NGB 85-09.
- NAGRA. 2002. Project Opalinus Clay: Safety Report – Demonstration of disposal feasibility for spent fuel, vitrified high-level waste and long-lived intermediate-level waste (Entsorgungsnachweis). Nationale Genossenschaft für die Lagerung Radioaktiver Abfälle Report, NAGRA Technical Report 02-05.
- NRCan (Natural Resources Canada). 2007. Canada's Nuclear Future: Clean, safe responsible. Natural Resources Canada news release 2007/50, June 14, 2007. (available at www.nrcan-rncan.gc.ca/media/newsrelease/2007/200750.e.htm).

Nuclear Waste Management Organization (NWMO). 2005. Choosing a way forward. The future management of Canada's used nuclear fuel. Nuclear Waste Management Organization. (Available at www.nwmo.ca).

Nuclear Waste Management Organization (NWMO). 2009. Used Fuel Deep Geological Repository and Transportation System – Used Fuel Container Preliminary Design Requirements for the APM Update. APM-PDR-01110-0005-R00 Nuclear Waste Management Organization.

Olivella, S., Gens, A., Carrera, J., and Alonso, E. 1996. Numerical formulation for a simulator (Code_Bright) for the coupled analyses of saline media. Engineering Computations 13(7): 87-112.

SNC-Lavalin Nuclear Inc. 2010. Deep Geological Repository Design Report – Sedimentary Rock Environment. SNC-Lavalin Draft Report No. 020606-6200-REPT-000.